Fabrication and Characterization of Single-Strand Chitosan Fibers for Chitosan Hydrogel Scaffolds

Vahid Noohi

Mechanical Engineering Department
McGill University
Montreal, Quebec, Canada

April 2017

A thesis submitted to McGill University in partial fulfillment of the requirements of the degree of master of engineering.

To my Parents Ali and Nahid

for their unconditional love and support.

TABLE OF CONTENTS

ABSTRACT

Human voice is produced by self-oscillations of the vocal folds that consist two lips of soft tissue located within the larynx. According to the National Institute on Deafness and Other Communication Disorders (NIDCD), around 7.5 million people in the United States have difficulties for using their voices. Smoking, abuse of alcohol and caffeine, chemical exposure, laryngeal cancer, upper respiratory infection, and voice misuse are among patterns of risks that might lead to voice disorders. One common type of voice loss is vocal fold lamina propria (VFLP) scarring disorder. Injectable hydrogels (a gel composed of one or multiple polymers suspended in water) are proposed to potentially recover the elasticity of scarred VFLP. A biomimetic hydrogel based on glycol-chitosan is presently under investigation in the Biomechanics laboratory in the department of mechanical engineering at McGill University in order to treat VFLP scarring disorder. Cells within the chitosan scaffold tend to adopt a spherical shape, which hampers their mobility and movement. We hypothesized that the presence of fibers within the gel, make it possible for the cells to attach and spread along the fibers and migrate. Therefore, our objective in the study outlined in this thesis was to fabricate and introduce single-strand chitosan fibers into the chitosan hydrogel matrix to promote the migration and mobility of fibroblast cells within the composite gel. In order to fabricate the fiber, a mixture of chitosan and acetic acid was prepared. The fibers were fabricated via direct extrusion. The primary solution was injected into a bath of acetone using a syringe pump. Fibers with an average diameter of 50 µm were obtained through selection of a proper needle size. The viability and migration rate of human vocal fold fibroblasts (hVFF) were investigated to study the reaction of the cells to the presence of the fibers. The ultimate strengths of the fibers were quantified with performing tensile tests. The composition and the surface topography of the fibers were studied using a scanning electron microscope (SEM).

Swelling tests were performed to quantify the fibers' capacity to incorporate growth factors and drugs. The storage modulus of the composite hydrogels was measured using a torsional rheometer. Overall, the chitosan fibers were successfully fabricated and introduced to the hydrogel and the mechanical and biological properties of the hydrogel scaffold were enhanced significantly. The viability and migration tests confirmed that adding the fibers to the scaffold is a promising method to promote cell migration. The mechanical properties of the composite scaffold were enhanced as expected.

RÉSUMÉ

Les auto-oscillations des cordes vocales, deux lèvres de tissus souples situées au niveau du larynx, sont à l'origine de la voix humaine telle que nous la percevons. Selon l'Institut National De la Surdité et autres Désordres de la Communication (NIDCD), environs 7.5 million de personnes aux États-Unis ont de la difficulté à utiliser leur voix. La cigarette, l'abus d'alcool et de caféine, l'exposition à des produits chimiques, le cancer du larynx, des infections respiratoires, ou encore une mauvaise utilisation de la voix peuvent causer des troubles pathologiques de la voix. L'un de ces troubles est le trouble de cicatrisation de la lamina propria, un type de perte de voix commun affectant plusieurs personnes chaque année. L'injection d'hydrogels (composés d'une ou plusieurs polymères en suspension dans de l'eau) peut alors potentiellement permettre de retrouver l'élasticité du lamina propria endommagé. Un hydrogel biomimétique incluant du glycol-chitosan est actuellement à l'étude au laboratoire de biomécanique du département d'ingénierie mécanique de l'Université de McGill afin de traiter ce problème. Les cellules se trouvant au sein des hydrogels de chitosan homogènes tendent à avoir une forme sphérique, ce qui limite leur mobilité ainsi que leur mouvement. L'hypothèse est que la présence de fibres dans le gel peut permettre aux cellules de s'attacher et de se propager le long des fibres, avant de migrer. Par conséquent, l'objectif principal de l'étude suivante fut de fabriquer puis d'introduire des fibres de chitosan dans une matrice d'hydrogel, afin d'améliorer la migration et la mobilité des cellules de fibroblastes au sein du gel composite. L'addition de fibres de chitosan altère et modifie les propriétés physiques de l'hydrogel. En effet, les fibres étant integrées dans la matrice de gel, une matière composite est crée. Celle-ci combine alors les propriétés physiques de la matrice d'hydrogel et celles des fibres. Un mélange de chitosan et d'acide acétique fut préparé. Divers groupes, selon leur concentration en solution primaire, chitosan et acide acétique, ainsi que la taille des aiguilles utilisées, furent

étudiés. L'extrusion fut employée comme méthode de fabrication. La solution primaire fut injectée dans un bain d'acétone à l'aide d'une pompe à seringue. En d'autres termes, le solvant à base de chitosan fut injecté dans un bain sans solvant. Grâce à une sélection rigoureuse de la taille et de la longueur de l'aiguille, des fibres avec un diamètre moyen de 50 μm ont pu être obtenues. Les fibres furent fabriquées avec des dimensions largement supérieures à celles des cellules, afin de faciliter le mouvement de ces dernières. Elles furent par la suite segmentées et mélangées à la matrice de manière aléatoire. Afin d'étudier la viabilité, ainsi que la migration des cellules de fibroblastes de cordes vocales, la microscopie confocale fut utilisée. Des essais de traction furent conduits afin de pouvoir déterminer la résistance des fibres. La microscopie électronique à balayage fut utilisée afin d'analyser la composition et la topographie de la surface des fibres. Des essais de gonflement furent effectués afin de quantifier la capacité des fibres à absorber les facteurs de croissance et les médicaments. Des mesures rhéologiques de torsions ont permis de mesurer le module de stockage de l'hydrogel avec fibres incorporées. Les résultats furent par la suite comparés avec des donnés similaires de matrices pures d'hydrogel sans fibres. Les propriétés mécaniques et biologiques de la matrice d’hydrogel furent augmentées de manière significative. Les tests de viabilité et de migration ont confirmé que l’ajout de fibres pa la matrice est une méthode prometteuse pour promouvoir la migration des cellyles. Les propriétés mécaniques de la matrice composite furent augmentées comme prévu.

ACKNOWLEDGEMENT

I would like to thank my supervisor professor Luc Mongeau for giving me the opportunity of working in his group. His strong support throughout my research, as well as his wise ideas and comments, made this study an enriching experience. I am grateful for the opportunities I was given to acquire new skills such as advanced microscopy.

I am very thankful to professors Francois Barthelat and Hojattolah Vali for granting me access to their equipment. Professor Barthelat generously provided me access to his lab and machine for performing tensile tests and professor Vali helped me access scanning electron microscopy (SEM) at the Facility for Electron Microscopy Research (FEMR) at McGill University.

I would also like to thank my colleagues and friends in the biomechanics lab at McGill University who made this journey pleasant especially Neda Latifi for her constant feedbacks.

I am sincerely grateful towards the people who patiently spent time guiding and training me on different equipment, machines, and experimental procedures: Annie Hélène Douillette (Biomechanics' lab manager), Roberto Martini (Laboratory for advanced materials and bio-inspiration lab manager), Dr. David Liu (Staff scientist at FEMR facility), Dr. Erika Wee (ABIF facility manager), and Rebecca Deagle (ABIF microscopy specialist).

All confocal and scanning electron microscopies were conducted at McGill University's facilities. Confocal microscopy was conducted at the Advanced Bio-Imaging Facility (ABIF) and Facility for Electron Microscopy Research (FEMR) was used for scanning electron microscopy.

This work was financially supported by the National Institutes of Health (NIH) grants DC005788 (Mongeau, PI) and DC014461 (Jia, PI).

I would like to thank my family, especially my parents for their unconditional love and support which made this journey possible.

LIST OF FIGURES

LIST OF TABLES

LIST OF ABBREVIATIONS

VFLP: Vocal Fold Lamina Propria

SEM: Scanning Electron Microscope

FEMR: Facility for Electron Microscopy Research

ABIF: Advanced Bio Imaging Facility

NIH: National Institutes of Health

NIDCD: National Institute on Deafness and other Communication Disorders

FRPs: Fiber Reinforced Plastics

CFRPs: Carbon Fiber Reinforced Plastics

GFRPs: Glass Fiber Reinforced Plastics

DCA: Dichloroacetic Acid

CRT: Cathode Ray Tube

HVFF: Human Vocal Fold Fibroblast

PBS: Phosphate-Buffered Saline

SD: Standard Deviation

1 INTRODUCTION

1.1 VOICE AND VOCAL FOLDS

Human voice is the audible sound produced by flow induced self-oscillations of the larynx. Perceptual correlate of frequency (pitch), intensity (loudness), complexity (quality), and variation of pitch, loudness, and complexity (variability) are four voice parameters [1]. Normal voice has a pleasant quality, with no voice perturbations and atonality, proper pitch (based on age and gender), and suitable loudness (weak or loud based on communication environment); furthermore, satisfactory flexibility (based on feeling) and sustainability (based on social and professional needs) are also considered parameters of a normal voice [1].

Voice disorders are very common and can range from moderate to severe. Around six percent of adults and 12% of children encounter voice problems at least once in their life time [2]. Voice problems are more common among specific groups of people such as teachers (50%), and administrative assistants (33%) [2]. People who are experiencing a voice disorder have to deal and cope with emotional and economical complications along with their physical injuries. Despite the fact that significant progresses have been achieved in understanding and addressing voice disorders, many questions remain unanswered [3]. Limited knowledge of the mechanisms of cellular differentiation, as well as biomechanical properties of the vocal fold layers makes it difficult to diagnose and treat vocal fold injuries properly [3].

Phonation is one of the fundamental functions of the vocal folds [4]. The vocal folds (cords) are composed of mucous membrane and are located across the larynx from back to front. The location of the vocal folds within the larynx is shown in figure 1-1. A vocal fold consists of epithelial, superficial, intermediate, and deep layers [4]. The lamina propria contains superficial, intermediate

(mostly elastin), and deep (mainly collagen) layers [4]. Each layer has a different structure, and mechanical properties in order to optimize the functionality of the vocal folds [4].

Vocal folds' structural changes, might lead to irregular chaotic vibration, excessive tightness, modification of infraglottic airway, and alternation of their shape and mobility, leading to a voice disorder [1]. Figure 1-2 shows the layered structure of the vocal folds.

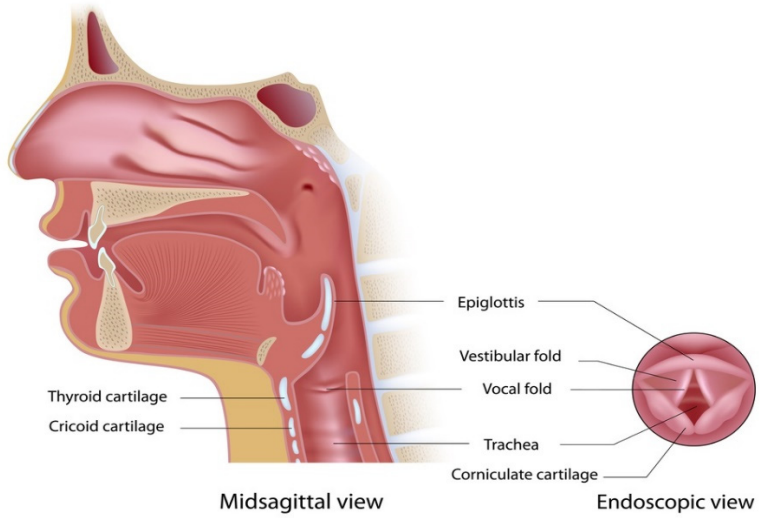

Figure 1-1-Vocal fold location in larynx-permission granted by Ray Schilling (NetHealthBook.com) [5].

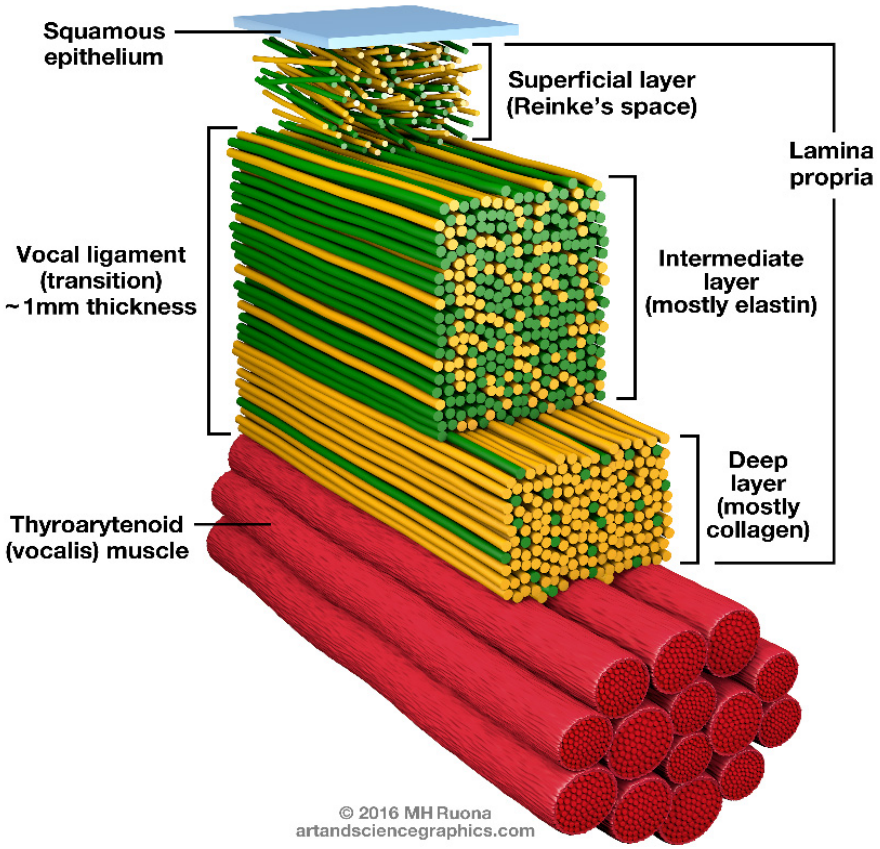

Figure 1-2-Diagram of the internal structure of the ligaments and muscles in the vocal folds in the larynx-permission granted by MH Rouna (artandsciencegraphics.com) [6].

Common voice problems are created by scar tissue in the vocal fold's vibrating layers [7]. *Scar* is characterized as a "disorganized structure or scaffolding" which results from body's effort to repair a wound [7]. Overuse of voice (in case of singers, teachers), aging, misuse of voice (wrong singing method), or abuse of voice (screaming) are common reasons for causing stress and "wear and tear" phenomenon leading to vocal fold injuries [7]. Voice disorders can be categorized into two main groups: '*organic type'* which includes dysphonias and aphonia resulting from mass lesions or neurological diseases and *'psychogenic type'* characterized with abnormal voice caused by psychoneurosis, and psychosis [8]. Dysphonias resulting from voice abuse is more common between children from ages six to nine, while both organic and psychogenic voice disorders target adults [8].

1.2 TISSUE ENGINEERING

Tissue engineering is a multidisciplinary field that includes material science, biology, engineering, and biochemistry. The goal of tissue engineering is to repair or even replace a diseased and infected biological tissue [9]. New and functional living tissues are generated by utilizing live cells along a matrix or scaffold to direct and cause tissue developments [10]. The loss or failure of a tissue that has been a serious challenge for the healthcare system is now addressed by tissue engineers to a great extent; however, some challenges remain that need to be addressed [11].

For this study, we targeted the vocal fold tissue, using the chitosan hydrogel as a matrix or scaffold, and investigated the reaction of human vocal fold fibroblasts (hVFF) to the gel.

1.3 BIOMATERIALS

The term *biomaterial* has been defined in several ways; in Merriam-Webster Dictionary, a biomaterial is defined as: "a natural or synthetic material (as a metal or polymer) that is suitable for introduction into living tissue especially as part of a medical device (as an artificial joint)", while Oxford Dictionary defines the biomaterial term as: "a biological or synthetic substance which can be introduced into body tissue as part of an implanted medical device or used to replace an organ, bodily function, ..."

Since the last century, the continued progress in designing and manufacturing of different materials has opened up many new opportunities in the field of biomedical sciences [12]. Metals, ceramics, polymers, and many other types of materials are widely used for biomedical applications. Implants, prostheses, and other medical devices are just a few examples of how biomaterials have revolutionized the field of biomedical sciences [12]. Successful use of biomaterials in human body is determined by properties of the material, design, fabrication method, and biocompatibility of the material of interest [13]. However, there are other factors beyond engineers' supervision that

influences the effectiveness of biomaterials, such as operation procedure, as well as patient's age, condition, and daily activities [13]. Some biomaterials, bioactive, cause an induction of biological reaction at the interface of the material making a strong bond between a tissue and the implanted material [14].

In this study, we used glycol-chitosan as a biomaterial for its biocompatibility, biodegradability, and healing activity.

1.4 CHITIN AND CHITOSAN

Chitin is the second most abundant polysaccharide in nature after cellulose. Biocompatibility, biodegradability, nontoxicity, inertness and toughness are among properties that make chitin a very good biomaterial for medical uses and in particular tissue engineering [15].

Chitosan (β-(1-4)- linked D-glucosamine and N-acetyl-D-glucosamine) is a linear polysaccharide soluble in many diluted acids. Chitosan, an important derivative of chitin, is industrially produced from shrimp or other sea crustaceans' shells [16]. Chitosan is also obtained by removing enough acetyl groups (CH_3CO) from chitin; a process known as deacetylation [16]. This process results in the release of amine groups (NH) changing the chemical state of chitosan to a cation [16]. Unlike chitosan, most polysaccharides are either neutral or negatively charged in acidic environments [16-23]. Figure 1-3 shows the chemical structure of chitosan.

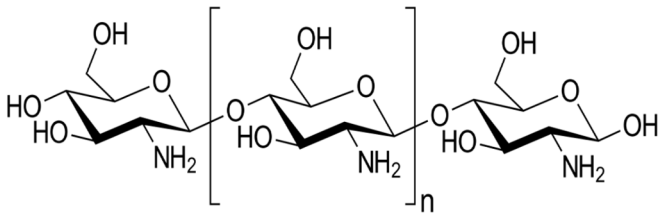

Figure 1-3-Chitosan chemical structure, Warraich Sahib, Wikimedia (https://commons.wikimedia.org/wiki/File:Chitosan_chemical_structural_formula.svg)[24].

In recent years, manipulation of chitosan's chemical structure has created unique functional characteristics in order to expand applications of chitosan within the biological and biomedical fields [16, 25-64]. Table 1-1 summarizes different derivatives of chitosan [16, 21].

Table 1-1-Chitosan Derivatives[16, 21].

No.	Derivatives	Functional group
1	N-Acyl Chitosans	Formyl,acetyl,propionyl,butyryl,hexanoyl,octanoyl,decanoyl, dodecanoyl,tetradecanoyl,lauroyl,myristoyl,palmitoyl,stearoyl, benzoyl,lauroyl,myristoyl,palmitoyl,stearoyl,benzoyl, monochloroacetoyl,dichloroacetyl,trifluoroacetyl,carbamoyl, succinyl, acetoxybenzoyl
2	N-Carboxyalkyl(aryl) Chitosans	N-Carboxybenzyl,glycine-glucan(N-carboxymethyl chitosan), alanine glucan, phenylalanine glucan, tyrosine glucan, serine glucan, glutamic acid glucan, methionine glucan, leucine glucan
3	N-Carboxyacyl Chitosans	From anhydrides such as maleic, itaconic, acetyl-thiosuccinic, glutaric, cyclohexane1,2-dicarboxylic,phthalic,cis-tetrahydrophthalic,5-norbornene2,3-dicarboxylic,diphenic,salicylic,tri-mellitic, pyromellitic anhydride
4	o -Carboxyalkyl Chitosans	o -Carboxymethyl, crosslinked o -carboxymethyl
5	Sugar Derivatives	1-Deoxygalactic-1-yl-, 1-deoxyglucit-1-yl-, 1-deoxymelibiit-1-yl-,1-deoxylactit1-yl-,1-deoxylactit-1-yl-4(2,2,6,6-tetramethylpiperidine-1-oxyl)-,1-deoxy-6-aldehydolactit-1-yl-,1-deoxy-6-aldehydomelibiit-1-yl-, cellobiit-1-yl-chitosans, products obtained from ascorbic acid
6	Metal Ion Chelates	Palladium, copper, silver, iodine
7	Sernisynthetic Resins of Chitosan	Copolymer of chitosan with methyl methacrylate, polyurea-urethane, poly (amide ester), acrylamide-maleic anhydride

1.5 COMPOSITE MATERIALS

A composite material is composed of two or more materials which are different in terms of chemical and physical properties. After combination, the properties of the new product is completely different from initial individual materials [65]. For instance, wood is a natural

composite made of cellulose fibers held together by lignin (matrix). A reinforcement (fiber) and a binder (matrix) are two essential components of a composite material [65]. Stiffness and high strength are provided by reinforcing fibers. Glass, carbon, silicon carbide, alumina or alumina-silica compounds, and organic fibers are widely used [66]. Any material such as polymer, metal, or ceramic can serve as a matrix [67]. Polymer-based matrix composites are very popular due to the compatibility of this type of matrix with common fibers such as carbon or glass [67]. Some factors such as bonding between matrix and fibers, orientation of fibers, volume fraction of fibers, uniform distribution of fibers in matrix, solidification of matrix, and number of defects play vital roles in determining the overall properties of composite materials [67].

The following figure shows the relationship between the main engineering materials and their combinations [66].

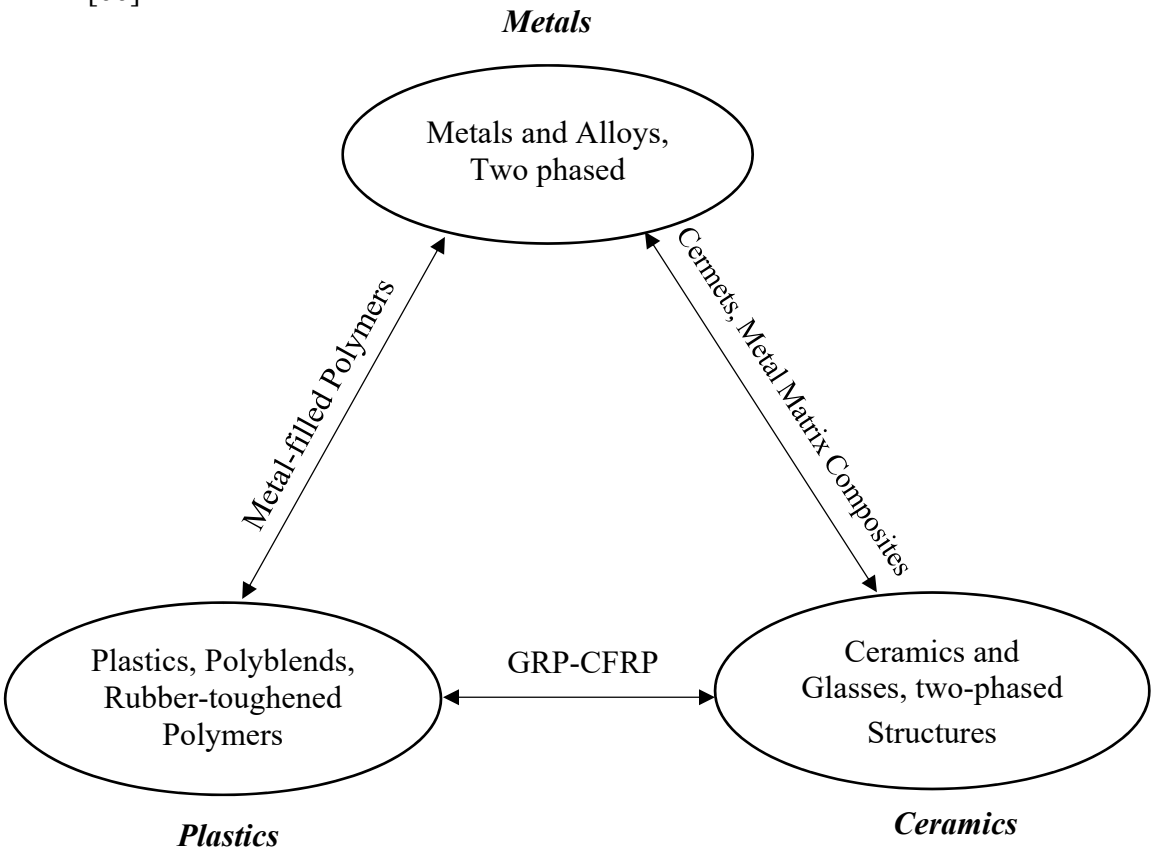

Figure 1-4-Relationship between engineering materials and obtained composite materials from these groups [73].

High specific strength, high specific stiffness, high damping, high corrosion resistance, and low coefficient of thermal expansion are some of the advantages that fiber reinforced plastics (FRPs), carbon fiber reinforced plastics (CFRPs), and glass fiber reinforced plastics (GFRPs) offer [68].

Composite materials in the biomedical field have served for various biological purposes; for instance, chitosan with alginate [69], collagen [70], calcium phosphate [62, 71], hydroxyapatite [72], and polysulfone [16, 73]. Yang et al. [74] reported a successful fabrication of porous hybrid scaffold for liver tissue engineering from alginate/galactosylated chitosan [75]. Nanoceramic composite scaffolds are capable to address bone cancer when bone cell division becomes irregular and out of control [76].

In this study, the chitosan fibers (reinforcement) were embedded in the chitosan hydrogel (matrix) to form a composite material (composite hydrogel).

1.6 FIBER FABRICATION METHODS

Extrusion and drawing are common methods for fabricating fibers. Extrusion is a process in which a billet is pressed through a die (orifice) under controlled conditions to fabricate a desired shape of a material [77]. In drawing, a billet is pulled through a die [77]. Fabrication in one pass, good surface finish, production of very large or small diameters of tubes and fibers, and great control on geometry and dimensions are among many advantages that the extrusion method offers [78]. Extrusion is categorized into two different types: hot and cold, which may be performed either direct (forward) or indirect (backward) [78]. In direct extrusion, a billet is pushed through a die to flow in the direction of a moving plunger (ram) while in indirect extrusion, a billet flows opposite to the direction of the motion [79]. Every year, almost 90 million tons of thermoplastics are processed with direct extrusion method due to its efficiency (little or no material is wasted) [80]. Direct (figure 1-5) and indirect (figure 1-6) extrusions are illustrated below.

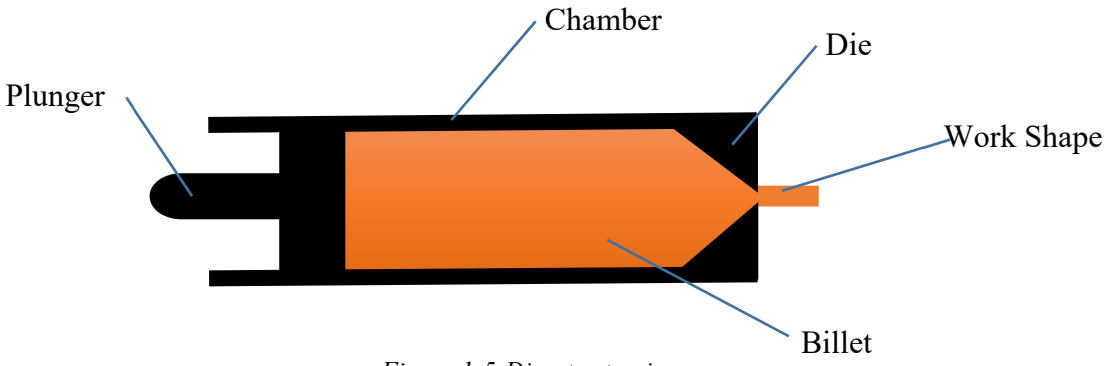

Figure 1-5-Direct extrusion.

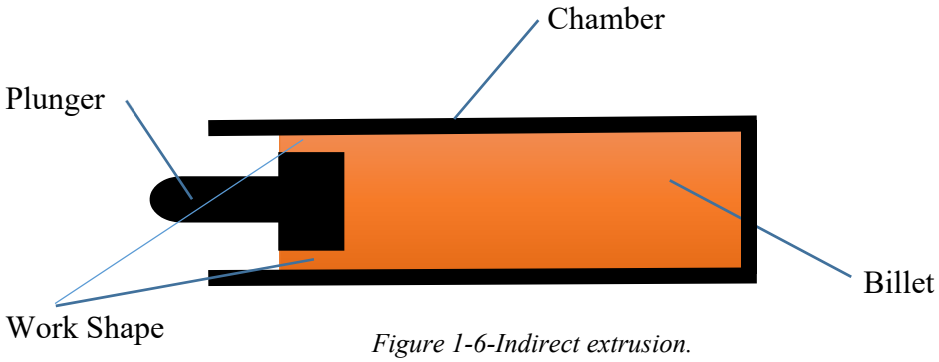

Figure 1-6-Indirect extrusion.

Direct extrusion was selected as the method of fabrication for the chitosan fiber in this study.

The first artificial fibers were fabricated in the nineteenth century from natural polymers (cellulose and casein) [81]. Natural polymers decompose instead of melting at elevated temperatures; therefore, production through using a melt (billet) is not feasible [81]. However, polymers and their modifications can be dissolved [81]. Evaporation and extraction are two common ways to remove the solvent [81]. Dry and wet spinning fiber formation are different based on the process of solvent removal [81]. In dry spinning, solvent is removed through evaporation, while in wet spinning the solvent is removed through extraction [81]. Highly viscous melt of thermoplastic polymers is also used for the fiber formation [81]. The only difference between fabrication from a solution and a melt, is the use of solvent in the polymer stream [81]. The presence of a solvent has

a significant effect on “unit” processes of fiber fabrication [81-88]. The relaxation time of polymers in solution is significantly shorter, which affects processing [81]. The crystallization process is another factor that is totally different in each method [81]. Depending on the concentration of the solution, the crystallization rate varies [81, 82, 85, 87, 88]. The crystallization of a polymer from a solution proves that it is very difficult to have low degree of crystallization in spun fibers, with the exception of some polymers that crystallize gradually and slowly [81]. It is very important to select a right solvent [81]. Some of the key points for selecting a proper solvent are: capability to form concentrated solutions, satisfactory heat stability, physiological idleness, and chemical inertness to the polymer which is dissolved (no crosslinking) [81].

The processes used for the spinning of synthetic fibers went through very significant modifications since their emergence, although, the core of the concept has not changed [89]. Many factors such as speed of spinning, the selection of the polymers, and processing methods have evolved [89].

2 LITERATURE REVIEW

In this section, previous studies on chitosan fiber fabrication are summarized.

One study conducted by Judawisastra et al. [90] reports that chitosan fibers were successfully fabricated using a laboratory scale wet-spinning device. The dope was made from 20g chitosan in 400 ml of 2% v/v aqueous acetic acid-methanol solution. Fibers were immersed into two different baths separately, one at the time. The first bath was prepared with 5L of NaOH 14% w/w at 50 ºC while the second bath contained 5 L of NaOH 2% w/w at 50ºC. The diameter of the fibers was reported to be between 364-460 µm with maximum tensile force between 5.6-8.3 N. Demineralization was controlled by temperature and time. The diameter of the fibers increased as the demineralization time rised. Upon extended demineralization, the density of the fibers and their

tensile strength decreased, however, their degradability increased. These results were obtained due to the reduced degree of crystallinity.

Another study was conducted by Tokura et al. [91]. For the chitin solution preparation, 5 to 7 grams of chitin powder was suspended in 100 cm^3 of 99 % formic acid at room temperature. The solution was frozen at -20ºC for 24 hours. After one day, the suspension was kept at room temperature to obtain a clear gel. The procedure must be repeated a few times. The gel was then dissolved in dichloroacetic acid (DCA). Isopropyl ether was added in the next step to lower viscosity. After filtering, the solution was spun. Table 2-1 shows the spinning conditions.

Table 2-1-Spinning Conditions for chitin by Tokura et al. [91].

Sample Number		31	56	79	80	61	62
Spinning condition	Solvent	FA-DCA (92:8)		FA-DCA-iPE (83:11:5)		FA-DCA-iPE (92:5:3)	
	Concn/%, w/v	3.0	4.0	3.8	3.8	4.6	4.6
Spinning Pressure		1.0-1.3($kgcm^{-2}$)					
Nozzle		Pt, 0.09 mmø-50holes					
Coagulation Bath	1st	EtOAc	iPE	Ace	Ace-iPE	EtOAc	EtOAc-iPE
	2nd	EtOH	50% AcOH:EtOH(2:5)			Cold Water	
Stretching Bath		Water(60ºC)					
1st roller/m min^{-1}		5.6	5.2	6.5	6.5	6.2	6.2
2nd roller/m min^{-1}		7.3	5.8	7.8	8.8	8.0	8.4
Elongation Ratio		1.32	1.10	1.20	1.35	1.29	1.35

-Solvent composition are volume ratio; FA: formic acid, DCA: dichloroacetic acid, iPE: isopropyl ether, EtOAc: ethyl acetate, Ace: acetone, AcOH: acetic acid, Cold water: 12-14ºC.

The key results of this study are summarized in table 2-2.

Table 2-2-Properties of chitin fibers by Tokura et al. [91].

Sample Number		31	56	79	80	61	62
Tenacity/g d $^{-1}$	Dry (20ºC,65% RH)	1.32	0.68	1.26	1.59	1.33	1.02
	Wet (20ºC,100% RH)	0.18	0.23	0.16	0.23	0.27	0.14
	Wet (90ºC,100% RH)	0.18	0.23	0.27	0.37	0.50	0.40
Elongation/%	Dry (20ºC,65% RH)	2.7	2.9	3.4	2.7	4.3	2.8
	Wet (20ºC,100% RH)	7.8	10.8	4.6	3.6	8.6	4.6
	Wet (90ºC,100% RH)	7.1	13.0	6.8	7.5	10.1	8.8
Knot strength/g d $^{-1}$		0.45	0.45	0.12	0.08	0.24	0.11
Density/g cm^{-3}		1.382	1.347	1.395	1.397	1.385	1.384
Moisture recovery/%		12.9	13.0	12.9	14.0	14.1	14.7
Denier/d		25.5	3.2	2.0	3.0	2.1	2.0

-RH: relative humidity.

Hirano et al. [92] investigated wet spun chemical N-modifications of chitosan-collagen fibers and their blood compatibility. Their study demonstrates that blood compatibility of chitin in combination with tropocollagen was enhanced. A mixture of chitosan and tropocollagen in aqueous 2% acetic acid-methanol (2:1, v/v) using a viscose-type spinneret was spun in a bath of aqueous 5% ammonia with 40-43% ammonium sulfate. Chemically N-modified chitosan and tropocollagen fibers were produced by applying of carboxylic anhydrides and aldehydes on the fresh fibers. The physical properties of three different types of filament (chitosan-tropocollagen, chitosan-collagen and chitosan) are reported in table 2-3.

Table 2-3-Physical properties of the filaments reported by Hirano et al. [92].

Filament	Tropocollagen (%)	Collagen (%)	Chitosan (%)	Titer (denier)[1]	Tenacity (g/denier)[1]	Elongation (%)[1]
Chitosan-tropocollagen						
108-1A	1	0	99	5.3±1.5	1.35±0.09	13.1±2.3
108-2A	2	0	98	13.8±2.8	1.65±0.38	12.7±4.5
108-3A	5	0	95	11.1±2.6	1.36±0.28	16.6±5.3
108-B-E[2]	5	0	95	23.8±7.0	1.21±0.39	22.3±12.7
108-B-P[3]	5	0	95	24.3±4.6	1.53±0.31	43.2±16.3
108-4A	10	0	90	6.2±0.76	1.33±0.24	15.9±1.5
145-1-3[3]	10	0	90	11.3±2.4	1.11±0.12	14.4±3.3
145-1-2	30	0	70	16.3±5.4	1.08±0.10	15.7±1.0
145-1-1	50	0	50	17.7±1.3	1.15±0.45	10.9±2.7
Chitosan-Collagen						
S-3[3]	0	2	98	21.3±3.9	1.21±0.11	11.1±3.6
108-C	0	2	98	13.0±1.0	1.37±0.08	17.4±6.5
S-2[3]	0	6	94	26.0±7.2	1.31±0.30	19.2±3.9
Chitosan						
145-1-4[3]	0	0	100	14.5±3.4	1.23±0.12	12.1±3.7
151-1-4[2]	0	0	100	14.8±0.76	1.10±0.16	9.9±3.8
151-1-5	0	0	100	4.0±1.7	1.11±0.10	13.4±2.8

(1)The average value of 3-6 analyses on the "filaments were conducted in this study.
(2)Without the stretching treatment in ethyleneglycol containing 2% NaOH, the "lament was air-dried without stretching.
(3)Without the stretching treatment in ethyleneglycol containing 2% NaOH, the "lament was air-dried with stretching.

N-substituted filaments from the chitosan-tropocollagen containing 5% tropocollagen (108-3A) properties, are reported in table 2-4. (3 to 6 analyses on the filaments).

Table 2-4-N-substituted filaments properties by Hirano et al. [92].

N-substituted Group	Titer (denier)	Tenacity (g/denier)	Elongation (%)
Acetyl	21.0±6.3	0.95±0.23	11.8±5.5
Propionyl	19.6±6.9	1.17±0.31	10.6±4.2
Butyryl	10.3±6.1	1.31±0.29	12.1±4.6
Hexanoyl	14.2±3.6	0.92±0.21	10.6±5.1
Succinyl	10.1±6.7	1.08±0.25	11.1±6.1
Benzylidene	10.5±4.1	0.86±0.28	8.0±5.0
Vanillin	5.9±1.6	1.01±0.34	8.7±6.9

Albanna et al. [93] investigated enhanced biological and mechanical properties of chitosan fibers. Chitosan was mixed with acetic acid in 0.01, 0.02, 0.03, and 0.06 volume concentrations to obtain 1.5% wt chitosan mixture. A 26G Teflon catheter was used for the extrusion. Two different ammonia baths with 10% wt and 25% wt concentrations were used to submerge the fibers. The fibers were left under tension for 15 minutes to be annealed by drying at 25,40,90,140, and 195ºC. Heparin was used as a cross-linker. The internal diameter of the Teflon catheter was 0.45 mm and the rate of extrusion was 85ml/min. In this group, one goal was to reduce diameter of the fiber in order to obtain a crystalline structure with higher strength. Increasing the concentration of acetic acid was found to increase the fiber's diameter. Dissolving chitosan in 2 vol% of acetic acid yielded fibers with optimal diameter and improved strength. Increasing the concentration of acetic acid (more than 2 vol%) yielded fibers with a larger diameter and a lower strength. Another factor affecting the chitosan fibers, was the concentration of ammonia. By increasing the concentration of ammonia, the diameter of the fibers was reduced due to higher crystallinity. Increasing the temperature while the fibers were left to dry was found to reduce the fibers' diameter and improve the mechanical properties.

Table 2-5 was prepared based on the reported data in this study (values are approximate).

Table 2-5-Reported results by Albanna et al. [93].

	Fiber Diameter (µm) 1vol%/2vol% AA	Tensile Strength (MPa) 1vol%/2vol% AA	Strain at Failure 1vol%/2vol% AA
10% Amm@25ºC	350/320*	0.7/1.2*	0.19/0.17*
25%Amm@25ºC	290/260*	1.2/2.3*	0..9/0.18*
25%Amm@195ºC	260/200*	2.3/4.1*	0.04/0.03*
25%Amm@195ºC+Hep	500/200*	0.2/4.9*	0.20/0.7*

-AA: Acetic Acid
- "*indicates p<0.05 between1and2vol%AA"

Glyoxal reaction as a cross-linker of chitosan was investigated by Qing Yang et al. [94]. Fibers were fabricated from chitosan powder and acetic acid solution (3.5% wt) through a spinneret.

Fibers were submerging in NaOH and Na_2SO_4. Glyoxal (cross-linker) effects were studied on the chitosan fibers by varying its concentration, temperature, and pH. Their finding reveals that the fibers which were cross-linked by glyoxal at 40ºC with a concentration of 4%v/v showed the highest (around 2.1) tenacity (cN/dte); in the first case, temperature and concentration were variables. Likewise, when pH of glyoxal was subject to change and close to 4 at 40ºC, tenacity was maximum (roughly 2.1). A tenacity of 2.1 was reached when fibers were cross-linked by pH of 4 for 60 minutes; time was a variable in this case.

3 RESEARCH OBJECTIVES

As it was mentioned earlier, a chitosan hydrogel scaffold is under development in the biomechanics laboratory at McGill University in order to treat and heal vocal fold lamina propria scarring disorder. Based on the previous experiments, this homogeneous hydrogel does not support cell adhesion and migration. Since the vocal fold structure is highly fibrous, we hypothesized the addition of synthetic fibers to the gel is a practical way for promoting cell adhesion and migration within the gel.

Fibers were selected to be examined for the stated purpose (cell mobility and migration) due to their: large aspect ratio (length over diameter), bending to very sharp radii, and numerous methods of fabrication [67].

Our objective in this study was to fabricate and introduce single-strand chitosan fibers for the chitosan hydrogel scaffold to promote the migration of the cells within the hydrogel, mimic in vivo conditions, and improve the mechanical viscoelastic properties of the hydrogel.

4 MATERIALS, AND FABRICATION METHOD

4.1 MATERIALS

We selected acetic acid (CH3COOH) to be the host solvent for glycol chitosan. Acetic acid is a very well-known solvent of chitosan. Glycol chitosan was selected since the hydrogel was developed from this type of chitosan. Figure 4-1 shows the chemical structure of glycol chitosan.

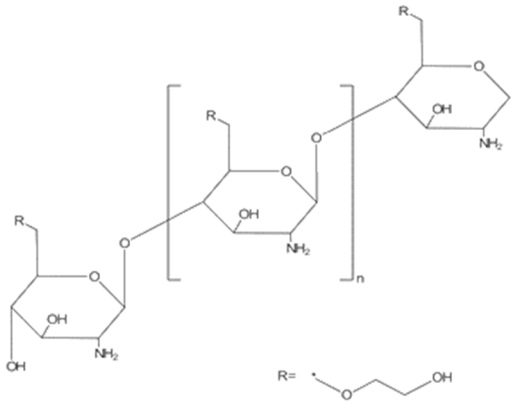

Figure 4-1-Chemical structure of glycol chitosan.

Acetic acid (A-300) was ordered from the ACP company in Montreal, Quebec with assay of 99.7% and LOT # J2015. Glycol Chitosan was purchased from SIGMA-ALDRICH with assay ≥ 60% (titration) (form: crystalline) and LOT#SLBP8298V. Acetone with assay of 99.7% and LOT# 164156 was obtained from Fisher Chemical. Glyoxal Solution (40% wt in H_2O) LOT# MKBV9169V was also purchased from SIGMA-ALDRICH. Ethyl Alcohol Anhydrous LOT#021331 was ordered from Commercial Alcohols company. Deionized Ultra Filtered water with LOT#164351 was obtained from Fisher. Phosphate Buffered Saline (PBS) 10x Solution with LOT#146393 was also purchased from Fisher. A LIVE/DEAD assay with LOT#1596086 was ordered from life technologies (molecular probes). Vybrant DiD Cell-Labeling solution from molecular probes was obtained.

Three different needle (Metal-flat tip) sizes were ordered from Hamilton Company to be examined for fabricating the smallest possible diameter (closest to the fibroblast cells' diameter). 21G (LOT#559589), 25G (LOT#558133), and 27 G (LOT#514396) needles were used in this study. 10mL Syringe with LOT#6146965 was purchased from BD company. 23 liters Autoclave model # 2540E was used from Tuttnauer company. Safe Seal 1.5 mL tubes with LOT#5177001 were obtained from SARSTEDT company. A µ-slide 8 well ibidi (uncoated and sterile) with LOT#160701/4 was used for imaging with a confocal microscope. An Eppendorf Repeater M4 dispenser with LOT#49820042191 was purchased. In this study, a NUAIRE biological safety cabinet and incubator (NU-5510/E) with 5% CO_2 and 37°C were used.

4.2 FABRICATION METHOD

A mixture of glycol chitosan and acetic acid with various concentrations (3%, 5%, and 7 % w/v) was prepared to be investigated. In order to do so, chitosan powder was first mixed with acetic acid to obtain the concentrations mentioned earlier. Then, the solution was placed on a rotating mixer for 72 hours to obtain a uniform mixture at room temperature. After 72 hours, a uniform yellowish solution was obtained. Next, a 10-mL syringe was used to extract the solution.

A bath of acetone was prepared to host the primary solution since acetone does not react with acetic acid and does not dissolve chitosan. Afterwards, the primary solution was injected into the acetone bath using a syringe pump. For this purpose, a New Era syringe pump (Model: NE-1000) was used and triggered manually for injection (extrusion). The injection was stopped whenever a target length was reached, to collect the fibers and resumed afterward.

The smallest fiber, with a mean diameter of 50 µm, was fabricated using the 27G needle. All preparation and fabrication steps were performed under a chemical fume hood.

Figure 4-2 shows the fabrication setup of the chitosan fiber.

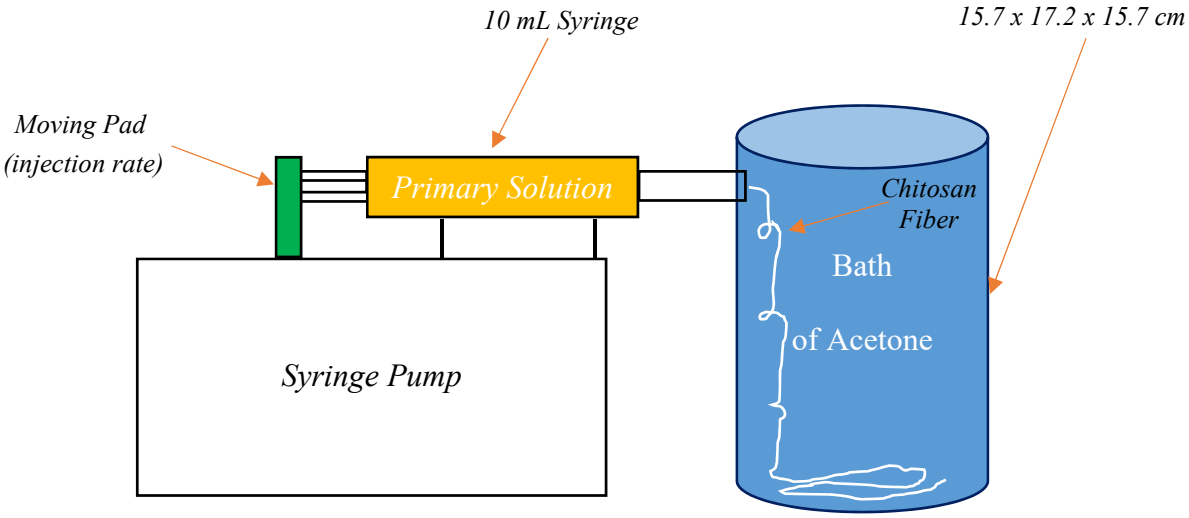

Figure 4-2-Setup for the fabrication of the chitosan fiber.

Figure 4-3 shows the actual setup which was used to fabricate the chitosan fibers.

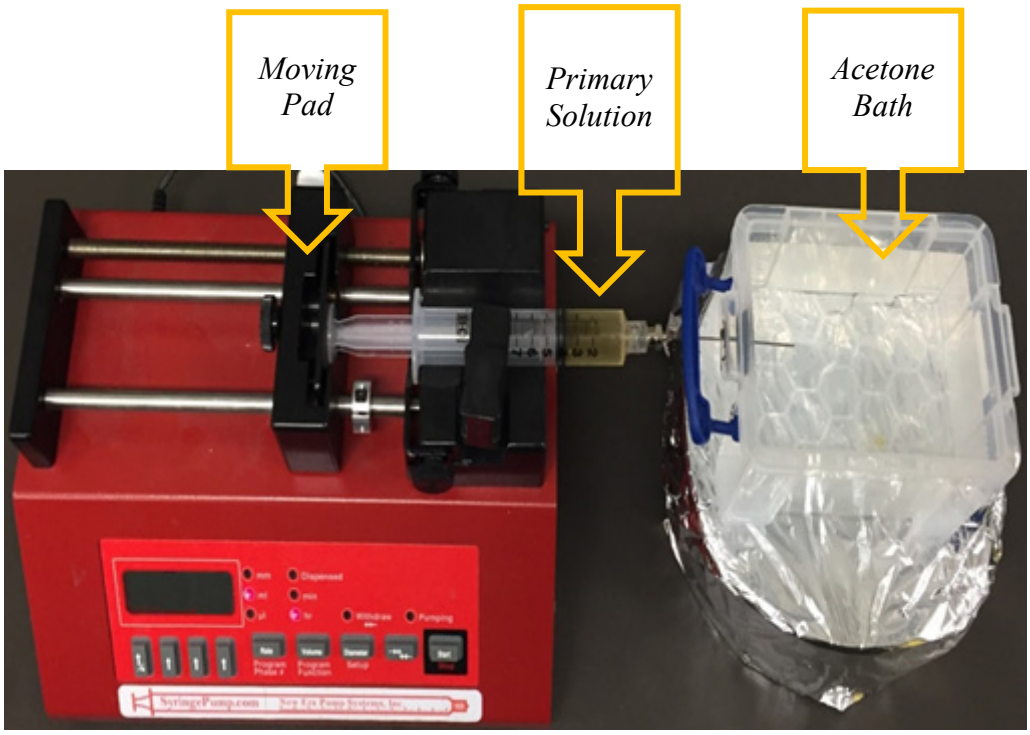

Figure 4-3-A schematic of the setup. A New Era syringe pump (Model: NE-1000) was used for injection (extrusion) of the primary solution (chitosan and acetic acid) to an acetone bath.

The topology of fibers was influenced by: the concentration of the primary solution, the rate of injection, the needle size, the solidification time, and the concentration of the cross-linker.

1- Concentration of the Primary Solution:

The concentrations of glycol chitosan in acetic acid were 3%, 5%, and 7% w/v in order to investigate how the viscosity of the primary solution affects the final product (fiber). At 3% concentration, no fiber was obtained due to the primary solution's low viscosity while the 7% w/v solution was too viscous to yield the desired outcome and caused blockage of the needle. The 5% v/w solution was found to be the optimal concentration for a successful fabrication.

2- Rate of Injection:

A rate of 20 mL/hour for injection of the primary solution into the acetone bath was selected through trial and error.

Rates lower than 20 mL/hour caused the primary solution to accumulate near the tip of the needle; therefore, hampering fiber creation, whereas higher rates than 20 mL/hour caused the primary solution to clog the needles.

3- Needle Size:

Three groups based on the needle sizes: 21G, 25G, and 27G were considered for this study. The minimum inner diameter of needle that could be used was 0.21 mm (27G). Needles with a smaller inner diameter were too fragile and easily blocked. The smallest possible fiber that was fabricated using the 27G needle, had a diameter of 50 μm (mean value). Table 4-1 shows the inner diameter of each needle and the diameter of the fabricated fiber using the same needle. Figure 4-4 is a schematic of the 27G needle.

Table 4-1-Needles and Fibers Diameter.

Group #	Needle Gauge	Needle Inner Diameter(mm)	Fiber Diameter(µm)
One	27G	0.21	50
Two	25G	0.26	75
Three	21G	0.51	129

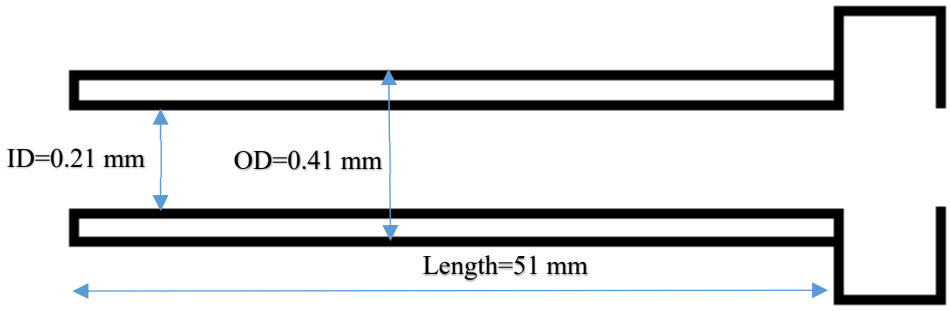

Figure 4-4-A schematic of the 27G needle.

4- Solidification Time:

After injection of the primary solution into acetone, the fibers were kept inside the acetone bath for 8 to 10 minutes. Afterwards, fibers were carefully removed from the bath using tweezers. The fibers were then dried for about 30 minutes at room temperature.

5- Cross-linker Concentration:

Glycol chitosan was tested and found to be soluble in water, therefore, crosslinking was required for the fibers in order not to be dissolved by cell culture medium. Glyoxal was chosen as the cross-linker since it was previously tested and used to crosslink the hydrogel. Since glyoxal is cytotoxic, it was used in very low concentrations to avoid cytotoxicity. Glyoxal, 40% wt., was diluted in 1x PBS. After preparation and examination of various concentrations, starting from 10%, 1% w/v concentration showed no cytotoxicity. Fibers were submerged in 1% w/v glyoxal for about five minutes to be cross-linked. Viability tests were performed to check and investigate the effects of the cross-linker on the cells (hVFF), which will be explained in details in the next chapter.

The fibers were sterilized and rinsed prior to coming into contact with the cells (hVFF). For this purpose, the fibers were submerged in ethyl alcohol anhydrous for about 15 minutes, then rinsed with deionized ultra-filtered water for 15 minutes in order to remove any residual stresses.

Figure 4-5 summarizes all the parameters that we considered for the fabrication of the chitosan fiber (figure 4-6) via direct extrusion.

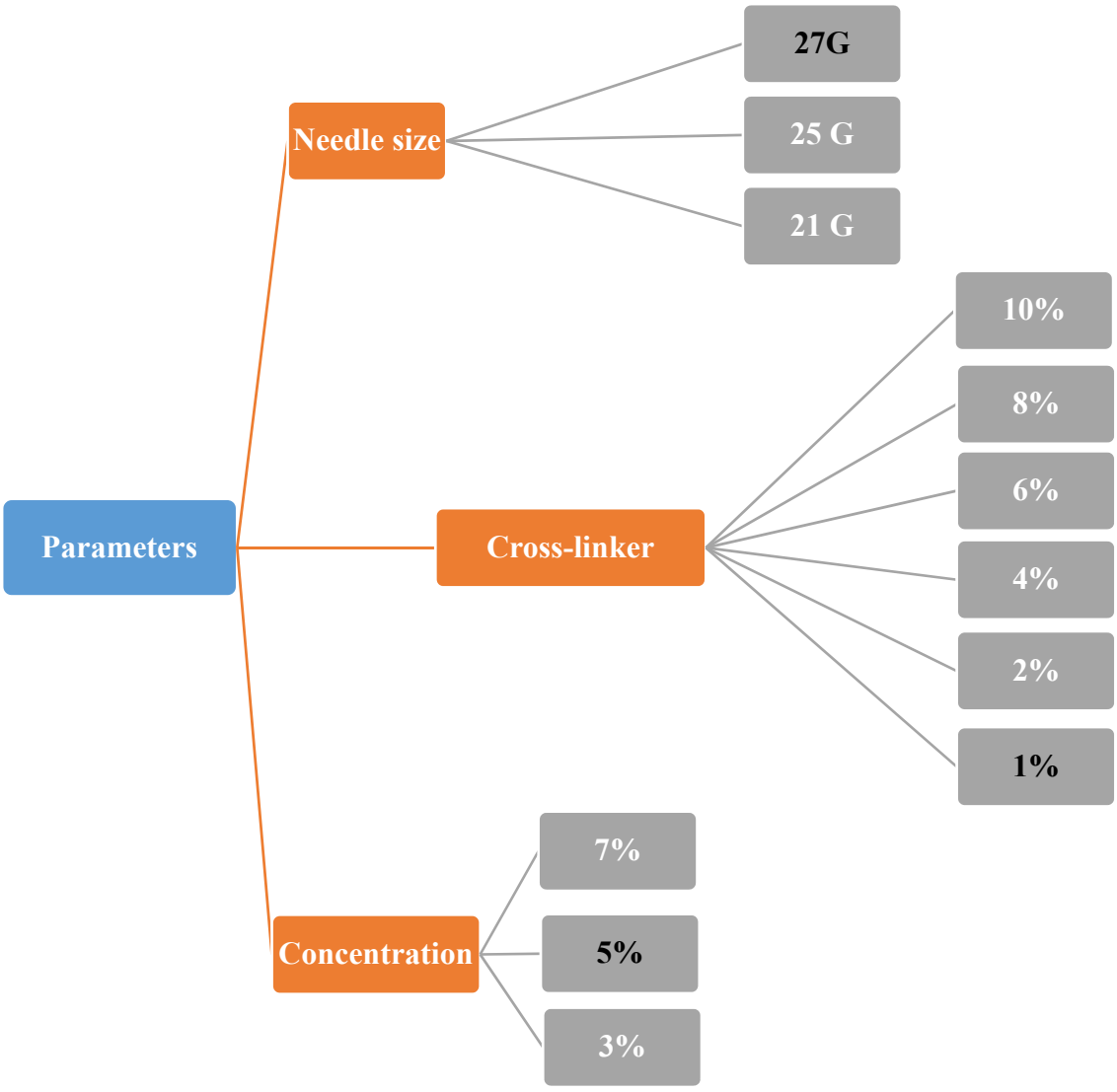

Figure 4-5-Parameters of the fabrication.

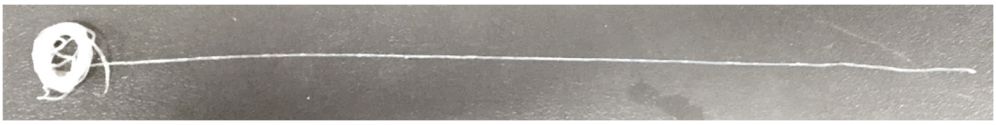

Figure 4-6-Chitosan fiber fabricated via direct extrusion.

An image of the fabricated fiber was captured with a Zeiss axiovert 200M fully automated inverted microscope in both Polarized and DIC modes with a magnification of 63x. In figure 4-7 the color difference indicates that the density is maximum at the center of the fiber.

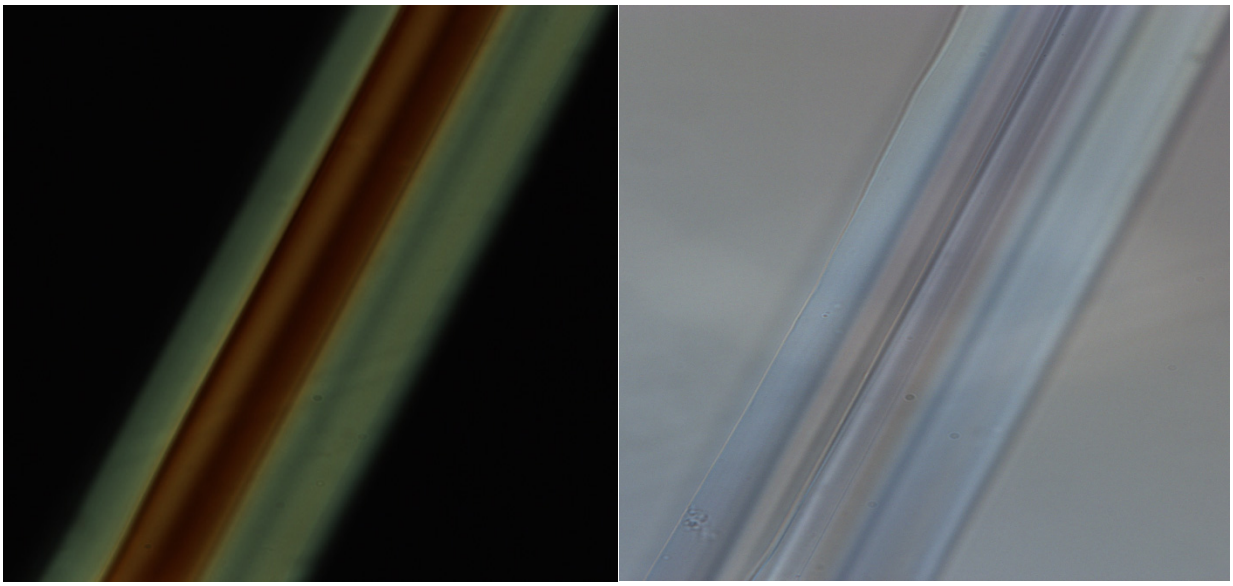

Figure 4-7-Chitosan fiber captured in Polarized (Left) and DIC(Right) modes using Zeiss axiovert 200M fully automated inverted microscope.

5 CHARACTERIZATION OF THE FIBER

We performed various tests in order to characterize the chitosan fiber both mechanically and biologically. In order to do so, viability and migration tests were performed to investigate how fibroblast cells (hVFF) would react to the presence of the fiber. Tensile tests, rheology, and scanning electron microscopy (SEM) were performed to obtain the mechanical properties of the fiber. Moreover, swelling tests were carried out to evaluate the capacity of the fiber in absorbing liquids for drugs delivery applications.

5.1 BIOLOGICAL CHARACTERIZATION

5.1.1 VIABILITY

We performed viability tests in order to study the reaction and viability rate of the cells within the composite hydrogel. After fabrication, crosslinking, and rinsing the fibers, the chitosan hydrogel was prepared to encapsulate both hVFF and the fibers.

In order to prepare the hydrogel, 10x PBS was diluted in deionized ultra-filtered water to obtain 1x PBS. Chitosan powder was then dissolved in 1x PBS with the proper proportion to obtain a 5 % w/v mixture. Next, the solution was placed on a rotating mixer for 72 hours to be uniformly mixed at room temperature. The final solution was then autoclaved using pre-set cycle program ("Glasswares for non-medicinal liquids in open bottles and glassware") in a 2540E model with a cold cycle of 25 minutes and hot cycle of 17 minutes. Next, Glyoxal (40% wt in H_2O) was diluted in 1x PBS to obtain 0.1% w/v for crosslinking of the hydrogel. Diluted glyoxal was autoclaved using the same cycle.

Human Vocal Fold Fibroblasts (hVFF) which were cultured in advance, were used to prepare around 20 million cells.

The chitosan mixture, the cross-linker, and the cells were mixed in a safe seal (1.5 mL tube) promptly in order to obtain a uniform solution. Using Eppendorf Repeater M4 dispenser, the solution was transferred in a µ-slide 8 well (150 µL in each well) for analyzing. After transferring the solution into the dish, the fibers were immediately placed into the gel before the hydrogel was cured and hardened. The prepared samples were placed in an incubator to be cured for three hours. After curing, the samples' surfaces were covered with a cell culture media. The media was changed every other day to avoid dryness of the gel, and to maintain homeostasis of the cells. The samples were then imaged on day zero (the day of sample preparation) and day seven (one week after

sample preparation) using a confocal microscope. The sample for day zero was stained after three hours (after curing).

All steps for preparing the samples were performed inside a biological safety cabinet to minimize the risk of contamination.

Figure 5-1 shows the preparation of the sample for the viability test with encapsulated fibers and cells within the hydrogel.

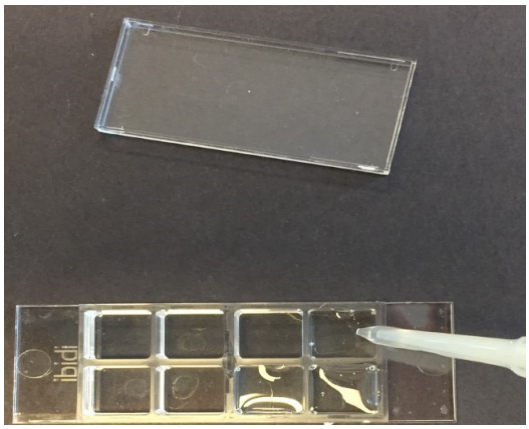

Figure 5-1-Preparation of the sample for the viability test in 8-well ibidi dish. The chitosan hydrogel, the cross-linker, and the fibers with embedded fibroblast cells were placed into the dish for confocal microscopy.

5.1.2 STAINING

Samples were stained for confocal microscopy using a LIVE/DEAD® kit for mammalian cells (Molecular probed life tech).

For the first step, all cell culture media was removed carefully using a pipetter. Each sample was washed with 1x PBS three time for five minutes each. Then, a solution of two milliliter 1x PBS (filtered), 4 µL component B from the kit, and 1 µL component A was prepared. The sample was incubated within the prepared solution (1x PBS + Comp. B + Comp. A) for 30 minutes. After incubation, the solution was removed and the samples were washed with 1x PBS three times for five minutes each. The sample was finally immersed in 1x PBS in order to maintain hydration

[95]. The stained cells were imaged at the microscopy center (ABIF) using a confocal microscope (LSM-710).

5.1.3 MIGRATION

The cells (hVFF) were first stained before getting encapsulated in the hydrogel for the migration test. The cells were suspended with the density of 10^6 /mL in a culture medium containing no serum. For every mL of suspended cell, 5 µL of the cell labeling was added. The solution was then mixed thoroughly. The labeled suspension was incubated for 20 minutes at 37 °C. The suspension was centrifuged at 1500 rpm for 5 minutes to separate cells from the rest of the solution. After removing the supernatant, the cells were suspended once again in the medium at 37°C (the last two steps were repeated twice) as recommended by the assay protocol [96].

After marking the cells, the procedure for preparation of the samples was exactly the same as the viability test.

5.2 MECHANICAL CHARACTERIZATION

5.2.1 TENSILE TESTS

Tensile (tension) test is a fundamental mechanical test which discloses important properties of a material. Ultimate strength, Young's modulus, and yield strength of a material are obtained by performing a tensile test. Young's modulus or modulus of elasticity is defined by the Hooke's law ($\sigma=E.\varepsilon$) which relates stress (σ) and strain (ε) of a material through the constant of proportionality, E (modulus of elasticity) [97]. Yielding occurs as soon as the linear relationship between stress and stain terminates [97]. Ductility, resilience, and toughness are other important mechanical properties that can be obtained by performing a tensile test. Tensile tests are mainly performed when a material is under development to reveal the behavior of a new material under uniaxial

tension or compression [98]. The results of a tensile test can be used to predict a material's behavior for an arbitrary loading [98].

We performed tensile tests in order to obtain the ultimate strength of the fibers. The ultimate strength is the capacity of a material to resist the maximum stress before failure [98].

In this study, the tensile tests were performed using a Fullam Inc. micro tensile machine. The process of fiber installation (mounting) on the machine was challenging since the fiber could easily slip due to its dimensions. In order to resolve this issue, sandpapers (150-grit fine) were used between the plates (where a specimen is installed) of the machine as shown in figure 5-3 to prevent the fiber from slippage. Pulling rate, and hydration of the samples had direct effects on the results. The rate of deformation, pulling, and the loading cell were 5 µm/sec and 4.54 kg (10 lbs.), respectively. The fibers were tested under three unlike conditions: dry and moisturized using two different liquids, which will be explained in details in the next chapter. Figures 5-2 to 5-4 show the setup for the tensile tests.

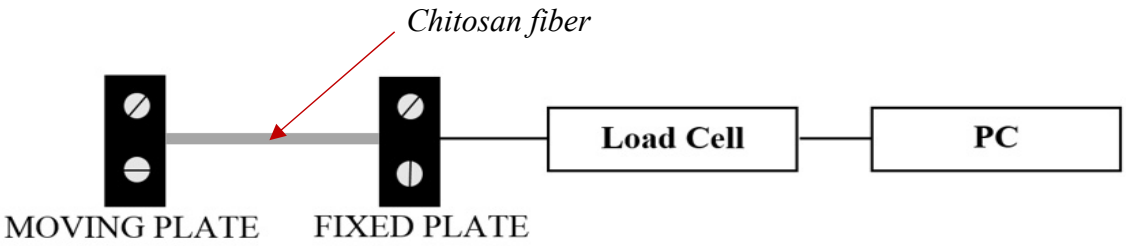

Figure 5-2-Top view of the tensile tests' setup.

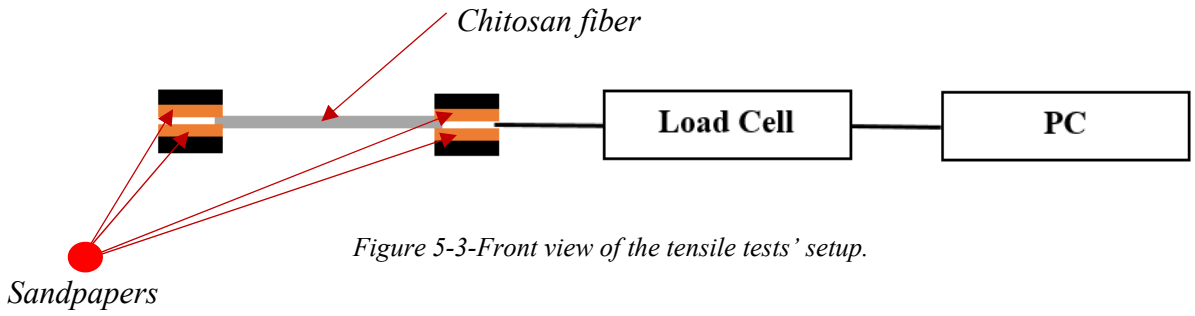

Figure 5-3-Front view of the tensile tests' setup.

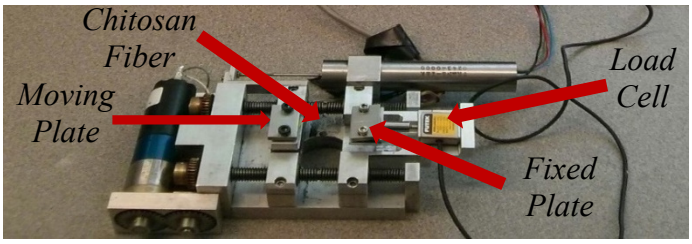

Figure 5-4-Photograph of the setup for the tensile tests.

5.2.2 RHEOLOGY

The investigation of deformation and flow of a matter is defined as rheology [99]. Rheology studies consist of viscous fluids and solids establishing viscoelastic or viscopalstic properties [100]. In the equation of $\tau=\mu\dot{y}$, shear stress τ (N/m^2) is proportional to shear rate $\dot{y}$ ($1/s$) with a viscosity μ (Ns/m^2) constant or function. Fluids that follow this linear relation are called Newtonian fluids and those that behave differently are considered non-Newtonians [100]. Rheology deals with the second group (non-Newtonian) of fluids which are highly viscous and exhibit elastic properties. Biological fluids, polymer solutions, and thermoplastics are among non-Newtonian fluids [100].

If viscosity of a fluid increases when shear rate rises, fluid is shear thickening. In contrast, if viscosity of a fluid decreases as shear rate increases, fluid is shear thinning. The following figure shows the relationship between viscosity and shear rate for different types of fluids.

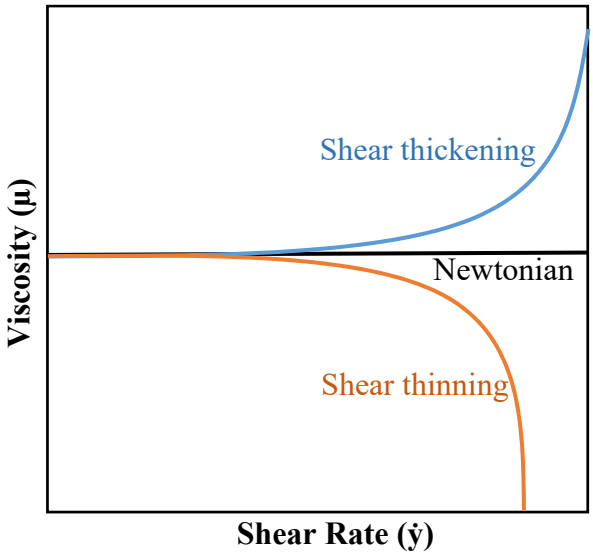

Figure 5-5-Relationship between viscosity and shear rate for different types of fluids.

There is a growing interest in using hydrogels for various tissue engineering applications due to their numerous advantages, such as injectability and continuous release of drugs [101]. In order to have a better understanding of these new hydrogels, the mechanical characterization is required [101]. Rheology is a suitable technique to be used for obtaining the mechanical properties of hydrogels since this method is relatively quick and reliable, and requires small samples for testing [101]. Useful information such as degree of crosslinking, glass transition point, and molecular weight can be obtained from data provided by rheology [101]. We used a torsional rheometer to obtain the storage modulus (log of Young's modulus) of the composite hydrogel.

For the rheology studies, the hydrogels were prepared as explained in section 5.1.1. The only difference in case of rheology, was using a custom-made mold with 20 mm diameter and 2 mm height for preparing the samples (hydrogel).

The fibers from each group, 27G, 25G, and 21G, were segmented and placed randomly in the hydrogel before letting it cure. Some samples were prepared without any embedded fibers as controls in order to be compared with the composite hydrogel groups.

We used a hybrid torsional rheometer (Discovery HR-2, TA instrument company) to carry out the rheology studies. Standard cylinder (Peltier Plate geometry) with a diameter of 20mm was obtained from the manufacturer. The rheometer (figure 5-6) and the test setup (figure 5-7) are illustrated below.

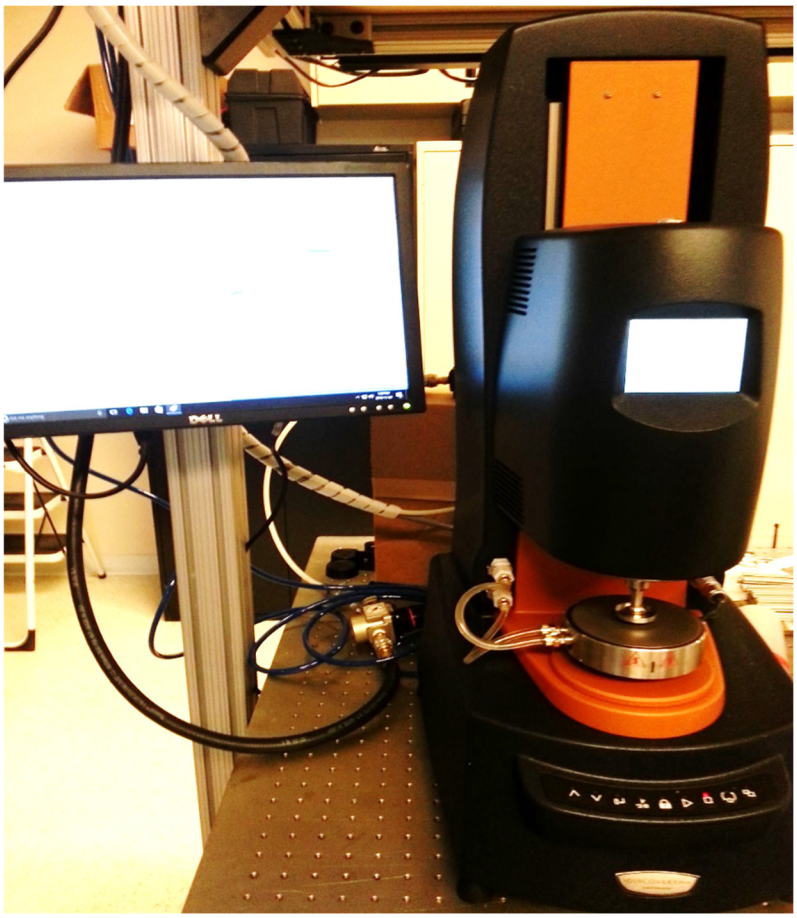

Figure 5-6-Hybrid rheometer (Discovery HR-2) used for rheology studies of the hydrogel.

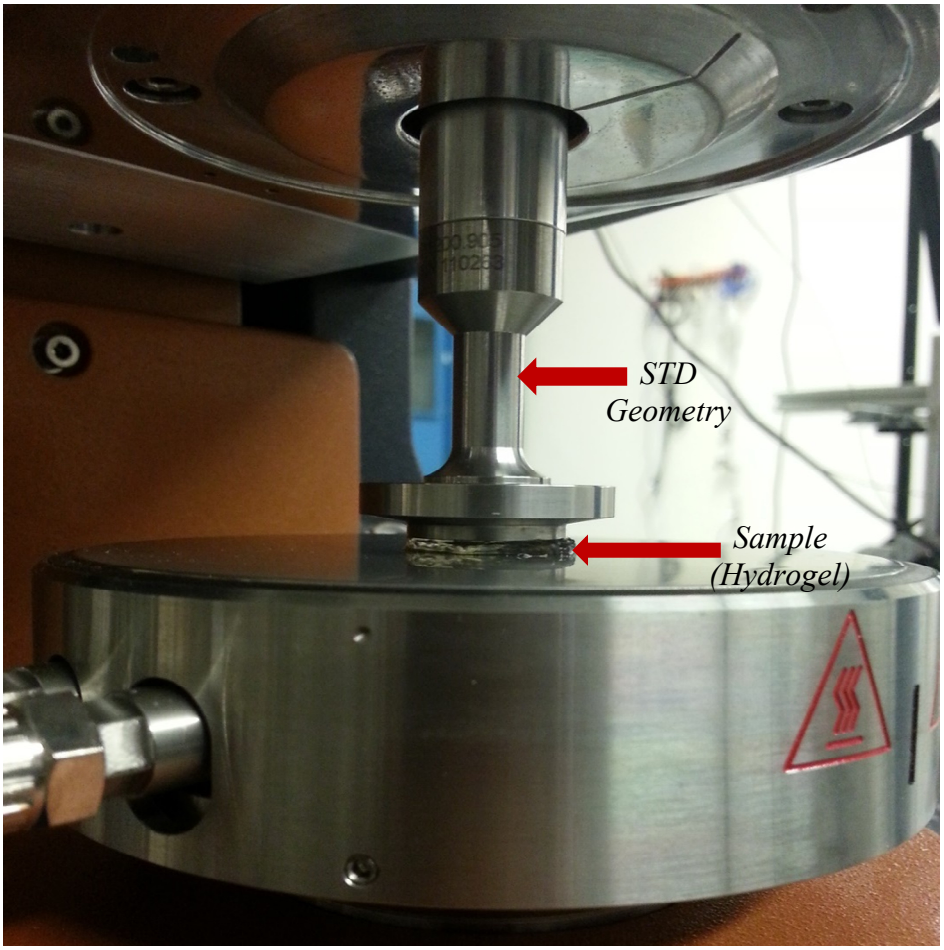

Figure 5-7-Hybrid rheometer (Discovery HR-2) with the loaded hydrogel.

5.2.3 SCANNING ELECTRON MICROSCOPY

Scanning electron microscope (SEM) is a flexible apparatus that is used to examine and study microstructure morphology as well as chemical composition of a sample (product) [102]. In SEM, light source is replaced with a high-energy electron beam and focused electron beam is used in order to scan the surface of samples thoroughly, resulting in formation of large number of signals [102]. Produced electron signals are then transformed to visual signals illustrated on a cathode ray tube (CRT) [102]. Figure 5-8 is a schematic diagram of a SEM.

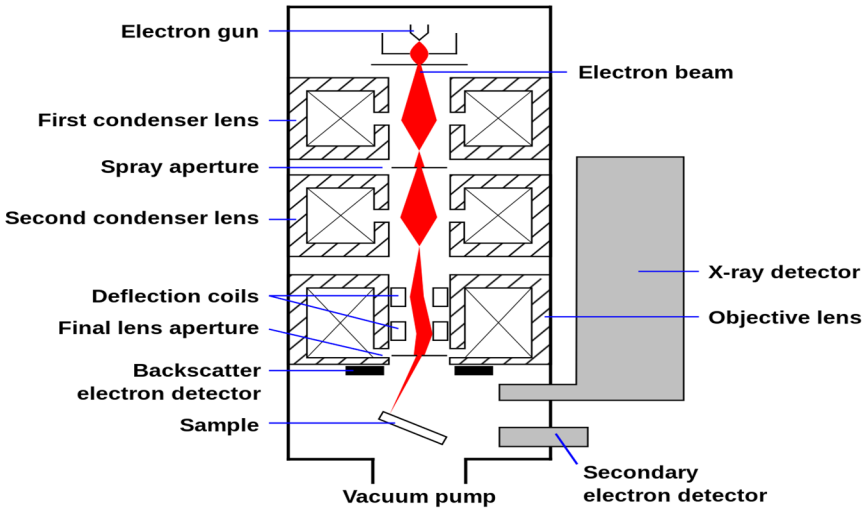

Figure 5-8-Schematic diagram of a scanning electron microscope, Schema_MEB_(it).svg, Wikimedia (https://commons.wikimedia.org/wiki/File:Schema_MEB_(en).svg.) [103].

We used a scanning electron microscope (SEM) to examine the surface morphology and to measure the diameter of the fibers in each group (27G, 25G, and 21G).

The chitosan fiber is not a good electrical conductor; therefore, a platinum coating was applied to prepare the fibers for scanning electron microscopy (SEM) using a Leica (EM ACE 600) coating machine (figure 5-9). The parameters of the machine for the samples coating are listed in table 5-1.

Table 5-1-Characteristics of the Platinum coating for the chitosan fiber.

Material	Current	Ar	WD	Tilt	Thickness	Sample height
Platinum	30mA	2.0E-2 mbar	45 mm	0°	4 nm	1 mm

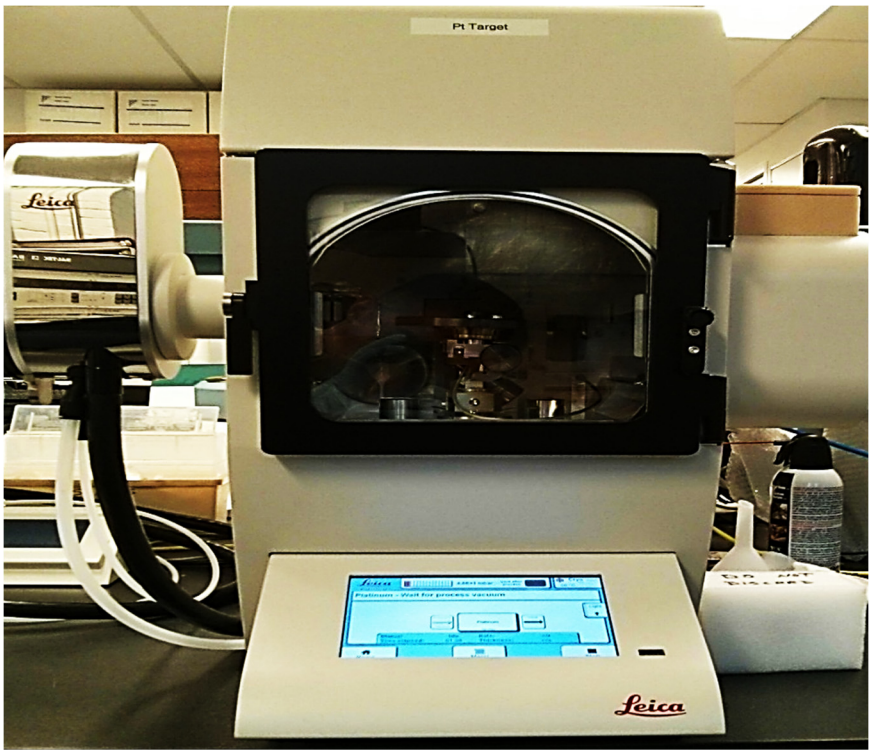

Figure 5-9-Sample preparation for the scanning electron microscopy. The chitosan fiber is not an electrical conductor and required a platinum coating.

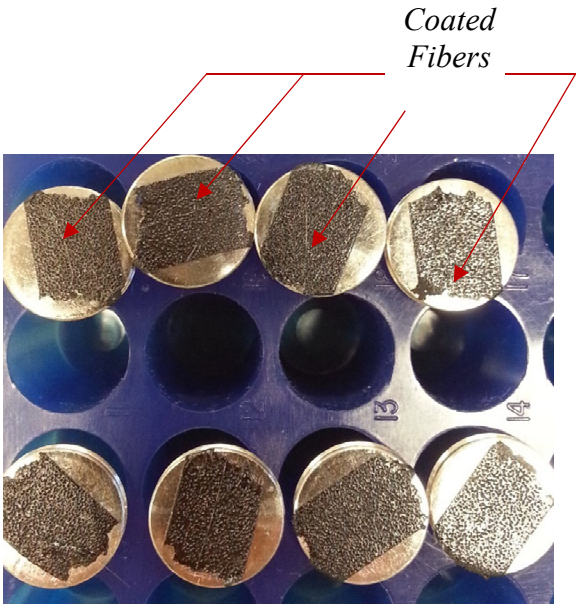

Figure 5-10-Samples were mounted on small pins to be coated with platinum.

After coating process, the FEI Inspect F-50 FE-SEM (EDAX Octane Super 60 mm^2 SDD and TEAM EDS Analysis System and iXRF XBeam XRF) machine was used to image the surface of the chitosan fibers. Figure 5-11 shows the scanning electron microscope which was used (F-50).

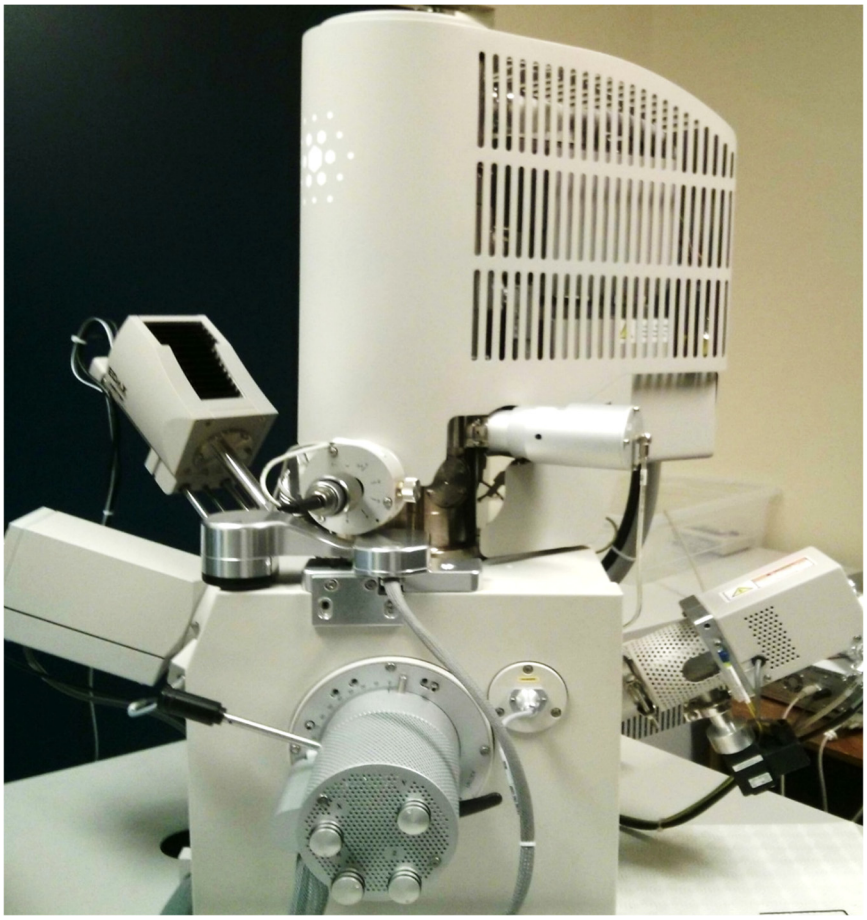

Figure 5-11-Scanning electron microscope (F-50) at the facility for electron microscopy research (FEMR).

5.2.4 SWELLING CHARACTERISTICS

Swelling or capability of expansion in polymers is determined through volumetric changes. We performed swelling tests in order to investigate the possibility of loading drugs or growth factors in the fibers.

For the swelling tests, weights of the empty vials were first recorded. Large number of fibers, due to their light weights, were placed in the vials and weighed. The fibers were submerged in 1x PBS

in order to assess their absorbance. The following time points were used: 4h, 24h,72h, 144h, and 168h. At each time point, 1x PBS was extracted using a syringe and after weighing, PBS was returned to the vial for the next time point. This procedure was repeated at all mentioned time points and weights were recorded for analyzing.

6 RESULTS

6.1 VIABILITY

As mentioned in section 5.1.1, the viability tests were performed at two different time points: day zero and day seven. The numbers of live and dead cells as well as the images that were obtained by a confocal microscope and processed using the IMARIS software are presented in tables 6-1 and 6-2, and figures 6-2 and 6-3, respectively. In figure 6-1, the difference between day zero (a) and day seven (b) results is shown.

Table 6-1-Number of live and dead cells for day zero.

Live Cells	Dead Cells	% Live
490	141	78
578	140	81
454	108	81
415	115	78
603	155	80
495	105	83
564	108	84
411	129	76
501	*125*	*Mean Value*

Table 6-2-Number of live and dead cells for day seven.

Live Cells	Dead Cells	% Live
247	170	59
511	389	57
237	188	56
450	247	65
351	221	61
662	352	65
534	329	62
375	229	62
421	*266*	*Mean Value*

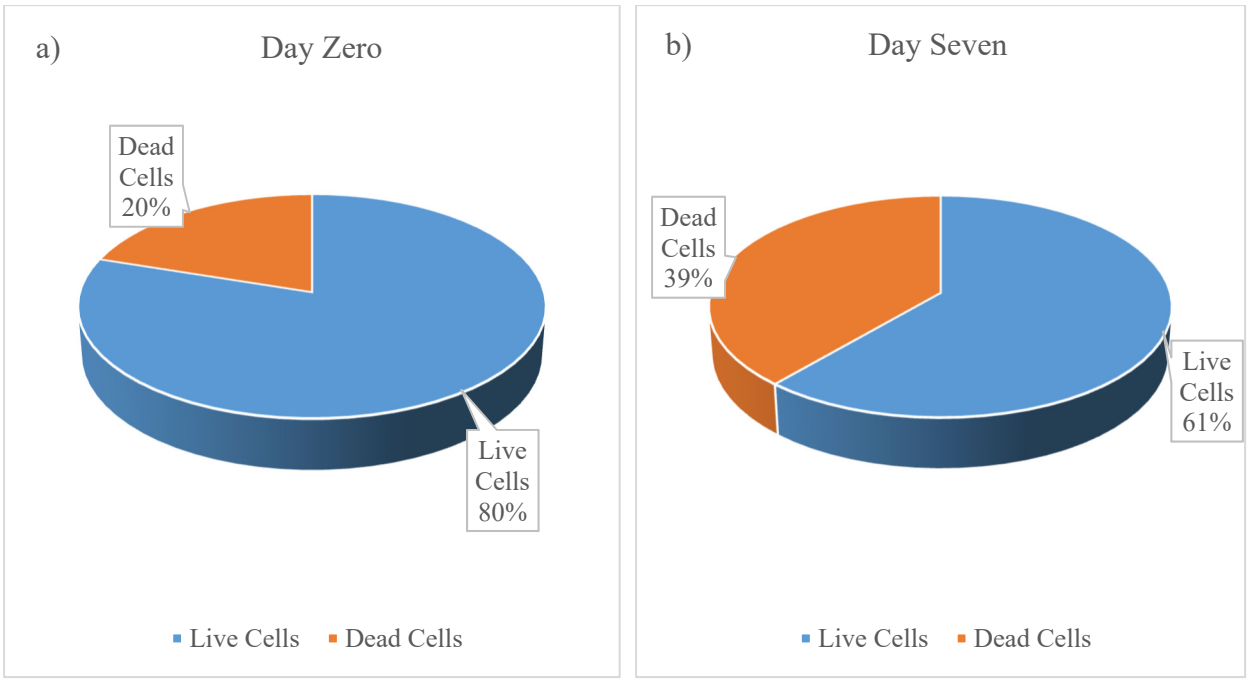

Figure 6-1-Pie charts to show the difference between a) day zero and b) day seven results.

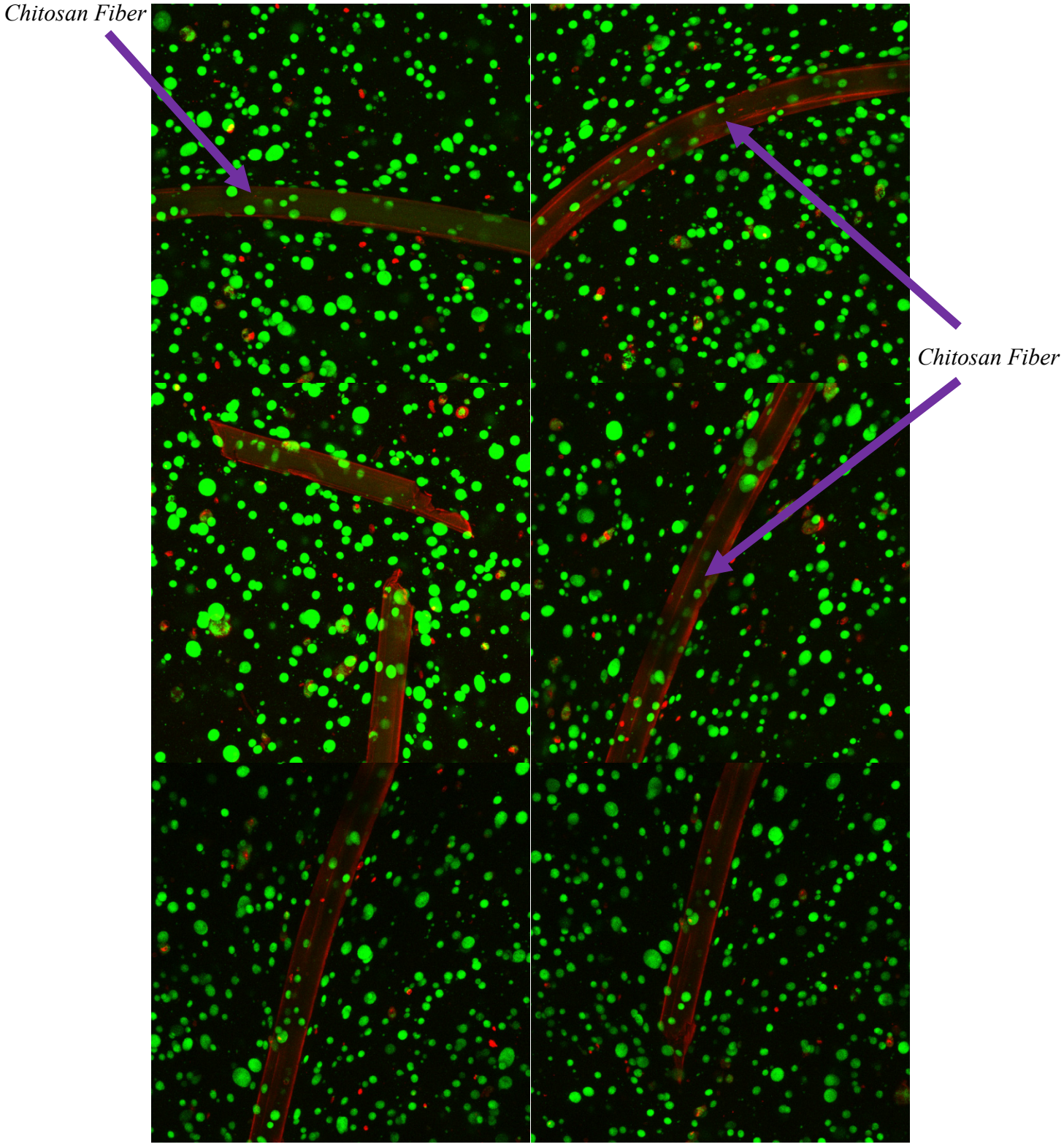

Figure 6-2-Viability test results. Live cells captured with the green channel and dead cells with the red channel using a confocal microscope for day zero. Human vocal fold fibroblasts were stained using the LIVE/DEAD assay.

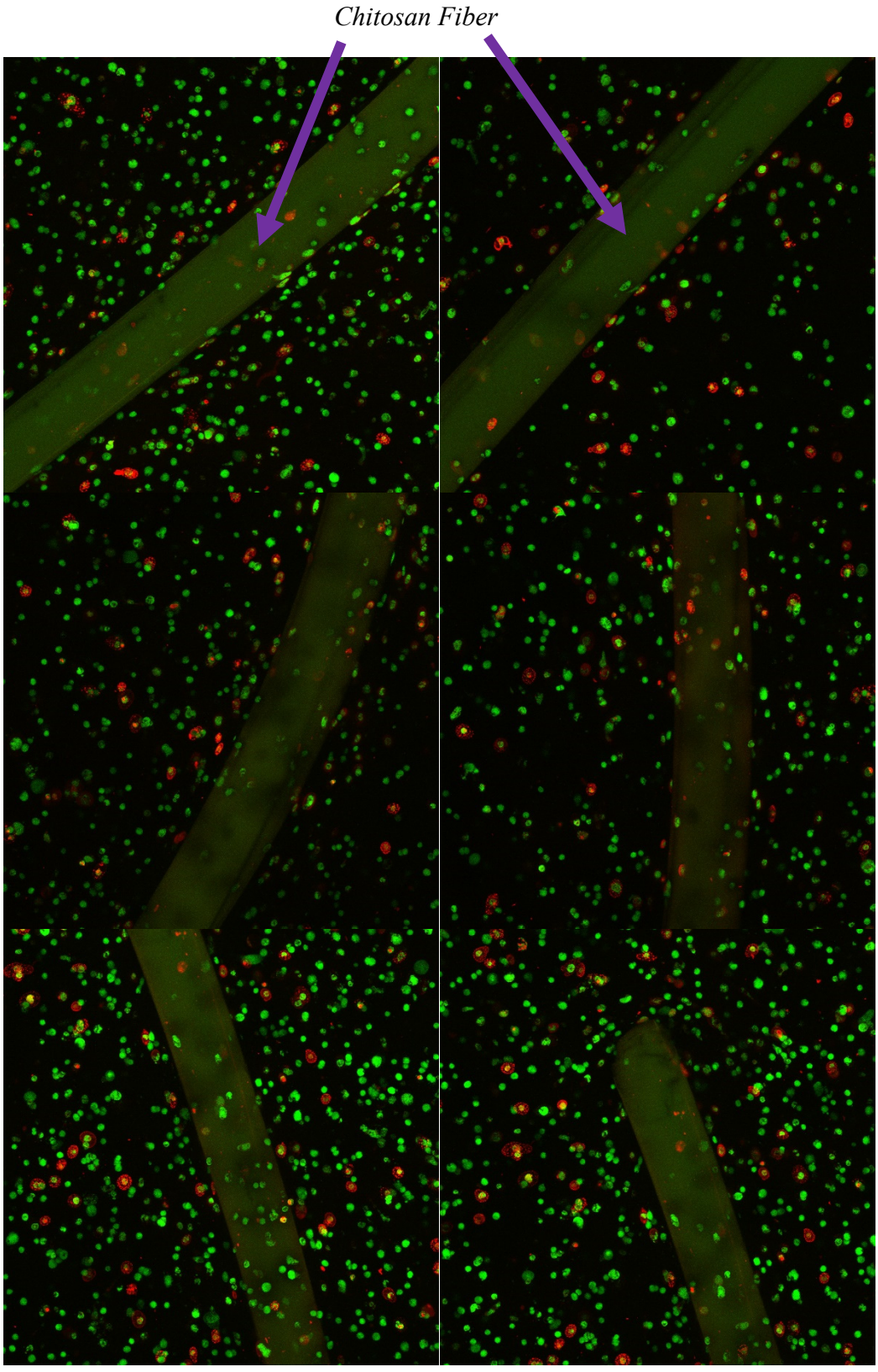

Figure 6-3-Viability test results. Live cells captured with the green channel and dead cells with the red channel using a confocal microscope for day seven. Human vocal fold fibroblasts were stained using the LIVE/DEAD assay.

6.2 IMAGE PROCESSING

We used the IMARIS image processing software (8.3.1 version) for post processing of the images. The surfaces were built and detected using the K-means clustering algorithm within the IMARIS software. The ratio of live to dead cells, as well as the area and the volume of hVFFs within the hydrogel were obtained. The results were exported in an excel sheet by the software. Figures 6-4 and 6-5 are the surfaces which were generated by the software for the post processing.

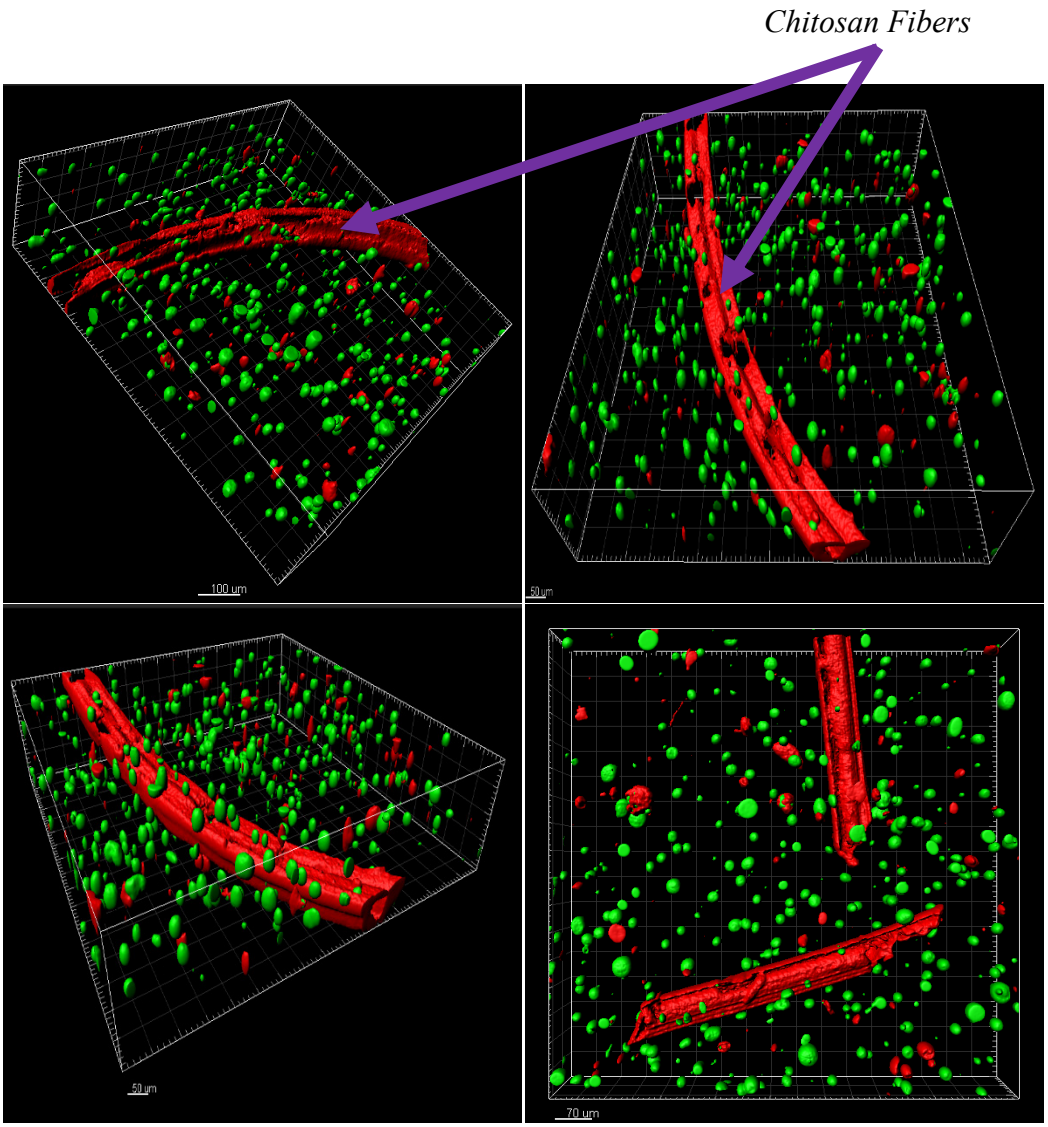

Figure 6-4-IMARIS software was used to analyze the viability tests' images for day zero. Live cells captured with the green channel and dead cells with the red channel.

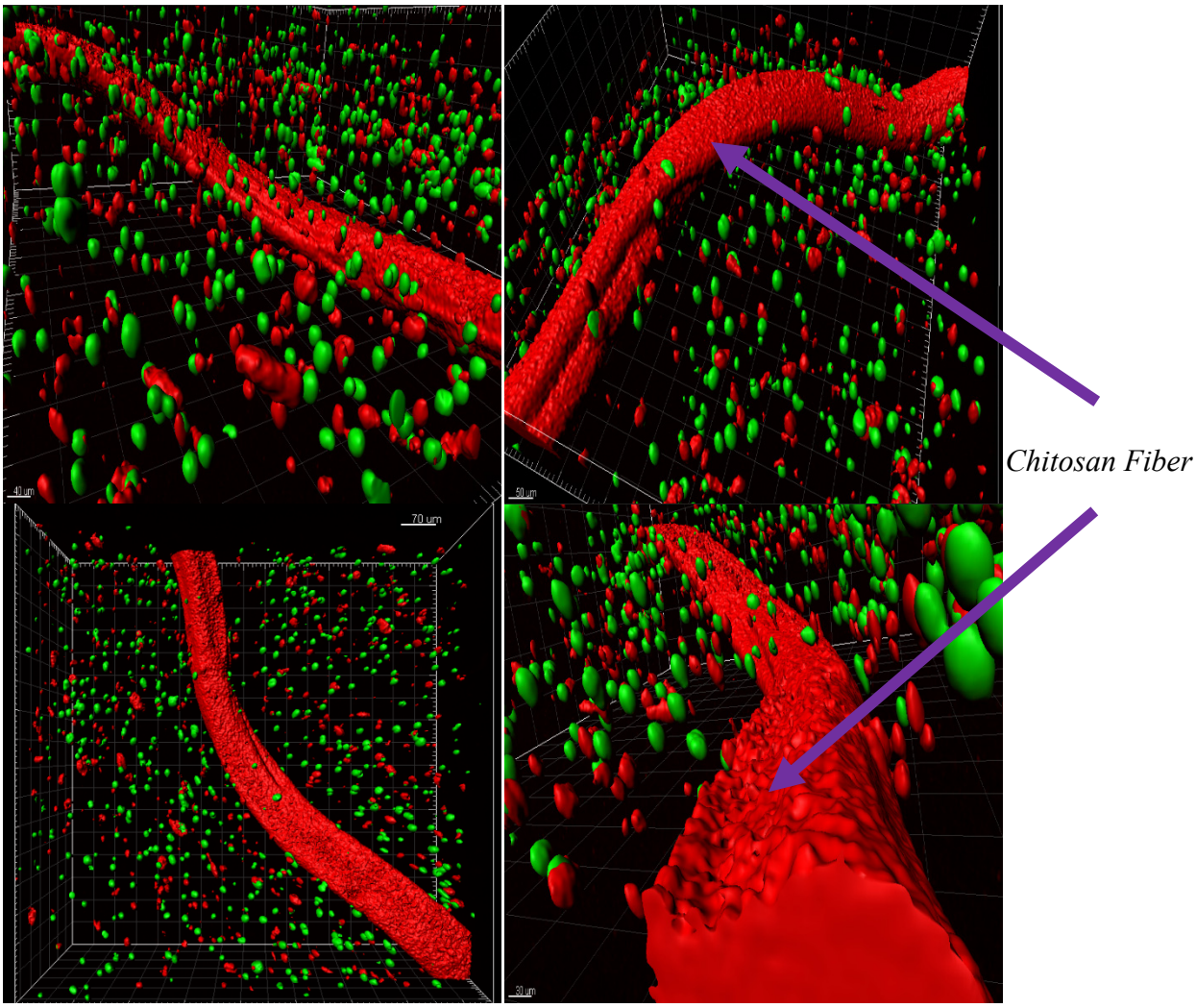

Figure 6-5-IMARIS software was used to analyze the viability tests' images for day seven. Live cells captured with the green channel and dead cells with the red channel.

6.3 MIGRATION

We investigated the migration of the cells within the hydrogel by encapsulating the cells in the hydrogel for 48 hours. The samples were then imaged for 18 hours. The movement paths of the cells were tracked using a confocal microscope and processed using the IMARIS software. Figure 6-6 shows the result of the migration test.

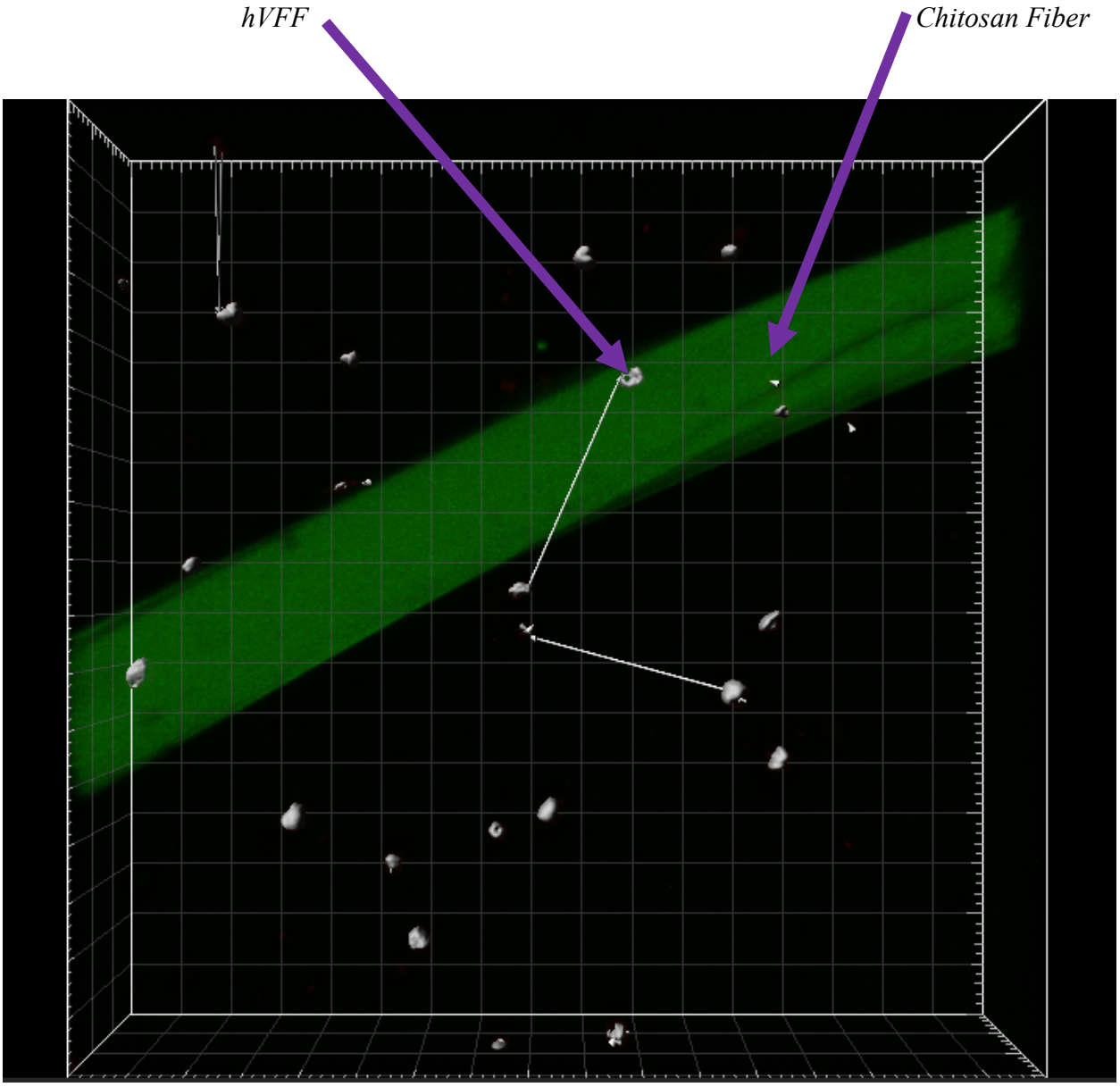

Figure 6-6-Migration test result processed by the IMARIS software. The white arrows were generated using the software indicating the path of the cells' movement.

6.4 TENSILE STRENGTHS

For the tensile tests, loads and positions were generated and exported by the software of the machine on an excel sheet. The stresses and the strains were then calculated based on the cross-sectional area and the initial length of the fibers, respectively.

Three unlike conditions were considered for each group (27G, 25G, and 21G) in order to study the behavior of the fibers under tension. First, some of the fibers from each group were tested in a dry condition at room temperature. For the second and third conditions, the fibers were moisturized

using water and 1x PBS, respectively. This was to determine whether the pH (water=7 and 1x PBS=7.4) of the liquid affects the performance of the fibers under tensile loading. Obtaining the ultimate strengths of the fibers for each group was the main purpose of conducting the tensile experiment. Error bars for the graphs are drawn based on the standard deviation (SD). The ultimate strengths of each group for the three conditions are shown in tables 6-3 to 6-5. In figures 6-7 to 6-9 the mean values of the ultimate strengths for the three conditions are separately plotted for each group. In figure 6-10 the ultimate strengths of the groups for the indicated conditions are compared.

Table 6-3-Ultimate Strength for the 27G.

DRY	PBS	WATER	
140.00	18.00	10.00	
163.00	13.00	10.00	
164.00	16.00	10.00	
172.00	16.00	14.00	
176.00	18.00	13.00	
163.00	16.20	11.40	Mean
13.96	2.05	1.95	SD
195.00	4.20	3.80	Variance

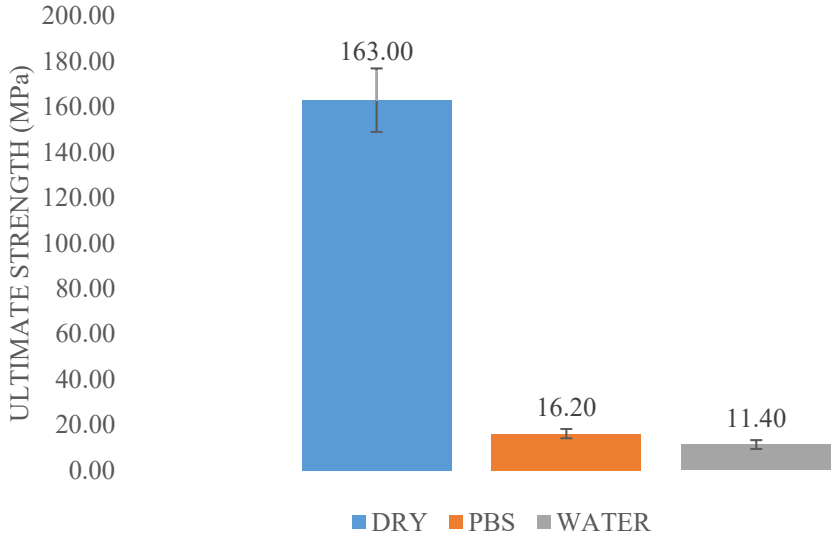

Figure 6-7-Ultimate Strength (mean) for the 27G group.

Table 6-4-Ultimate Strength for the 25G.

DRY	PBS	WATER	
100.00	15.00	9.00	
107.00	12.00	11.00	
127.00	16.00	11.00	
129.00	16.00	12.00	
133.00	18.00	12.00	
119.20	15.40	11.00	Mean
14.70	2.19	1.22	SD
216.20	4.80	1.50	Variance

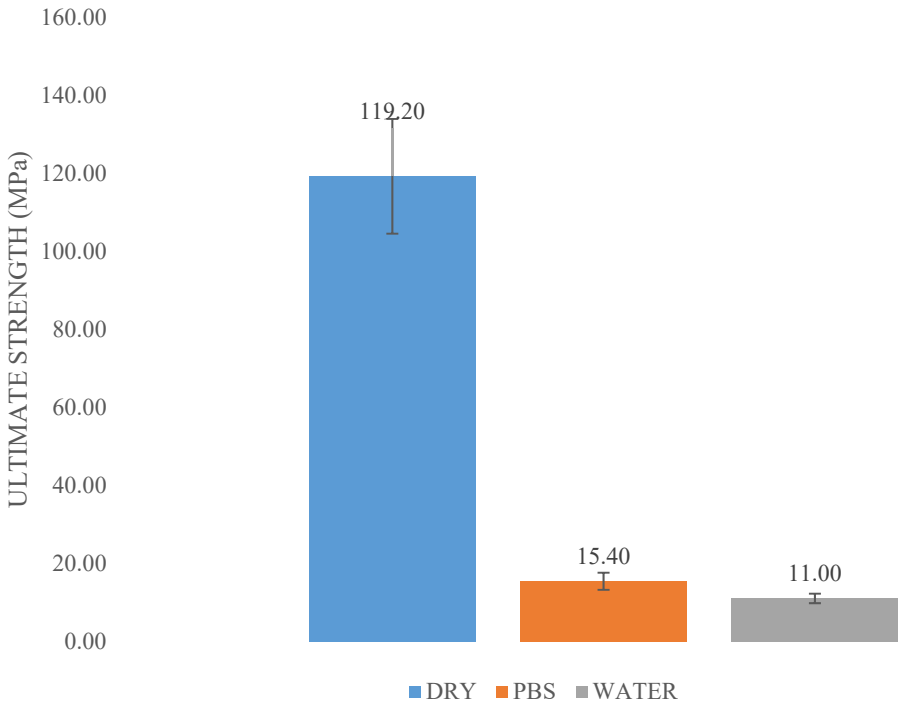

Figure 6-8-Ultimate Strength (mean) for the 25G group.

Table 6-5-Ultimate Strength for the 21G.

DRY	PBS	WATER	
81.00	11.00	11.00	
75.00	12.00	6.00	
76.00	10.00	9.00	
68.00	13.00	10.00	
68.00	15.00	10.00	
73.60	12.20	9.20	Mean
5.59	1.92	1.92	SD
31.30	3.70	3.70	Variance

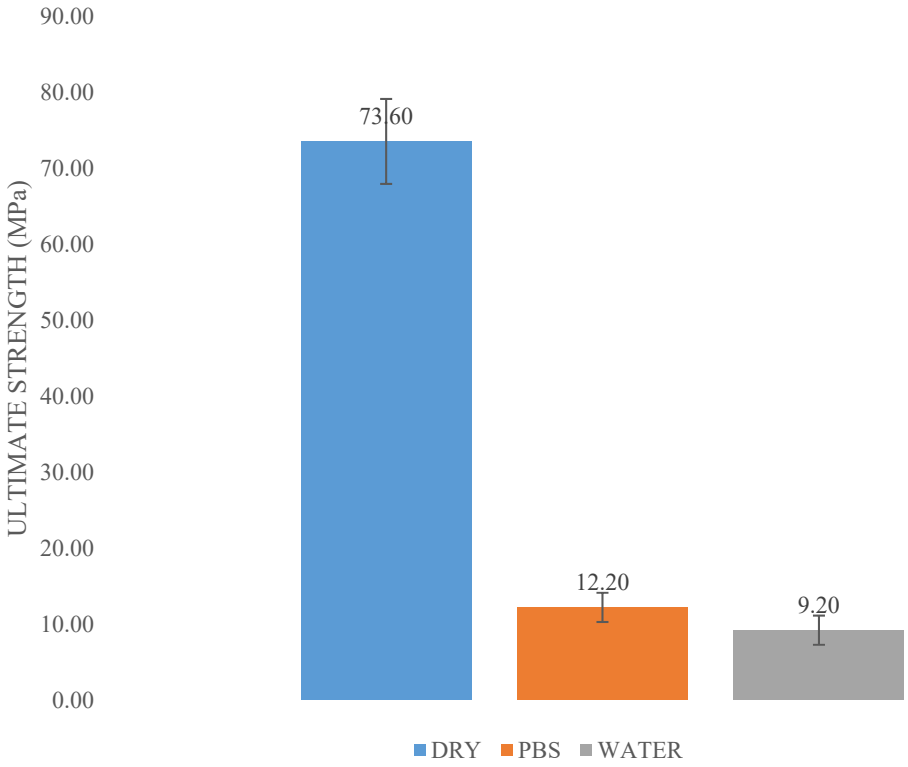

Figure 6-9-Ultimate Strength (mean) for the 21G group.

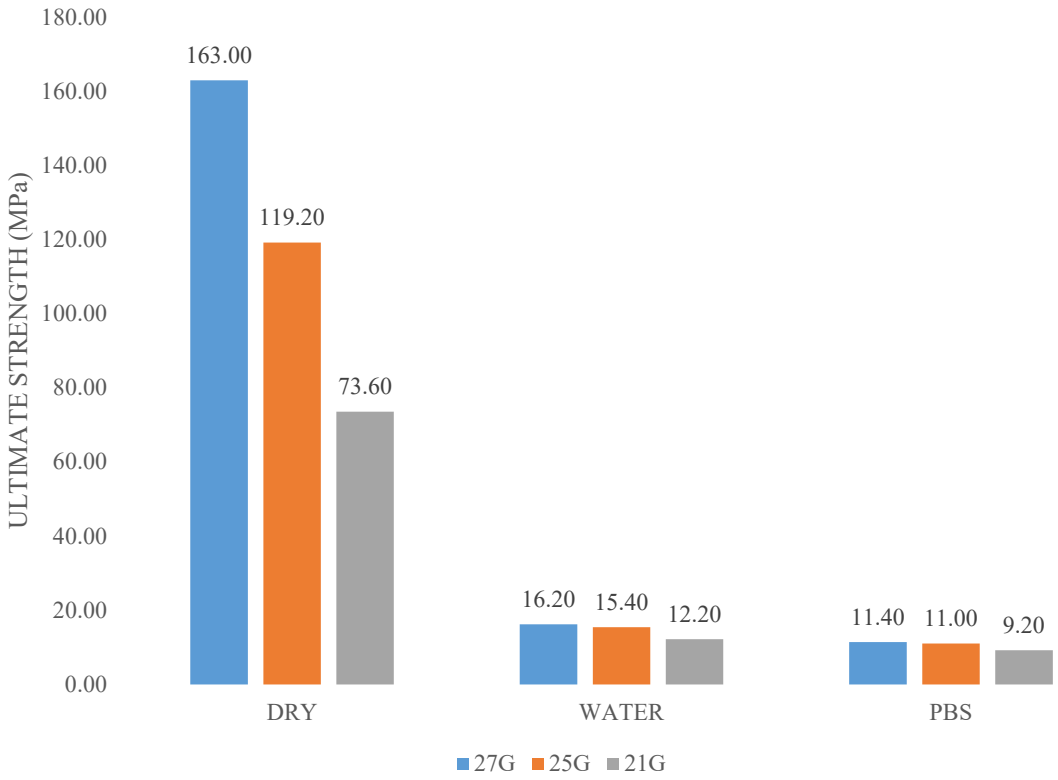

Figure 6-10-Ultimate Strength (Mean) for the three groups.

Table 6-6 shows the formulas that were used in order to calculate the stresses as well as the strains of the fibers. The stress-strain graphs for the three conditions (one graph for each condition) are shown in figures 6-11 to 6-13.

Table 6-6-Stress and strain formulas.

Stress:	Strain:
σ (Pa)=F(N)/A(m^3)	$\varepsilon=\Delta L/L_0$
σ: Stress F: Load A: Cross section area	ε: Strain $\Delta L=L-L_0$ L: Final length L_0: Initial length

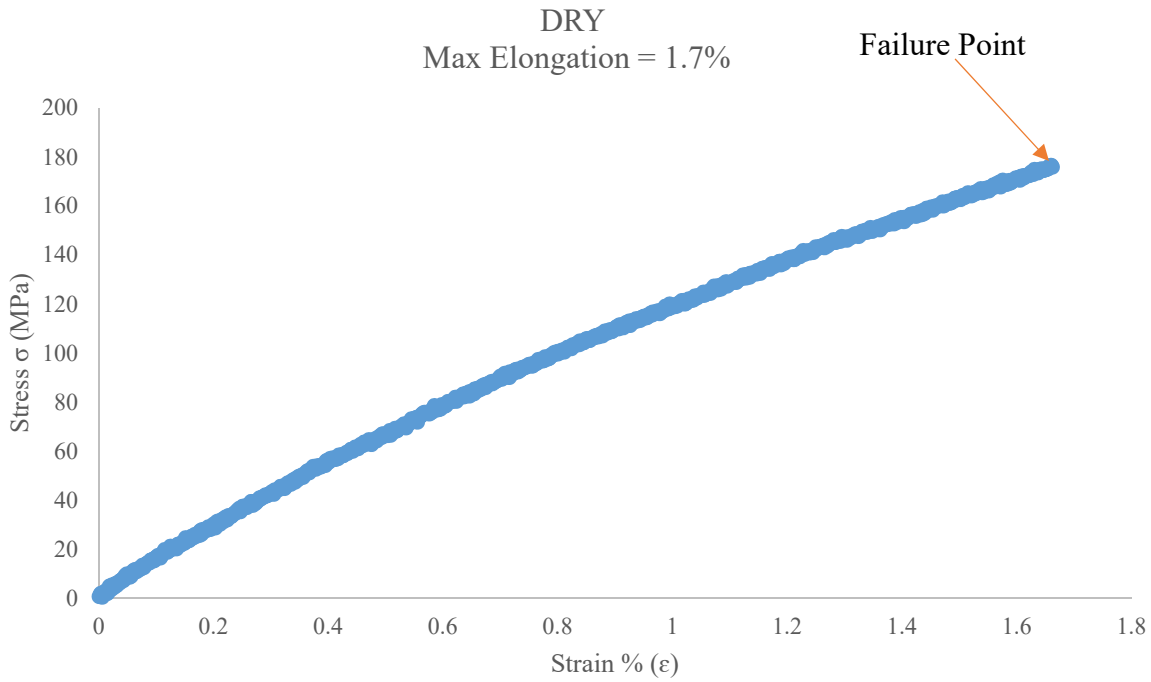

Figure 6-11-One example of the stress- strain curve of the chitosan fiber (dry).

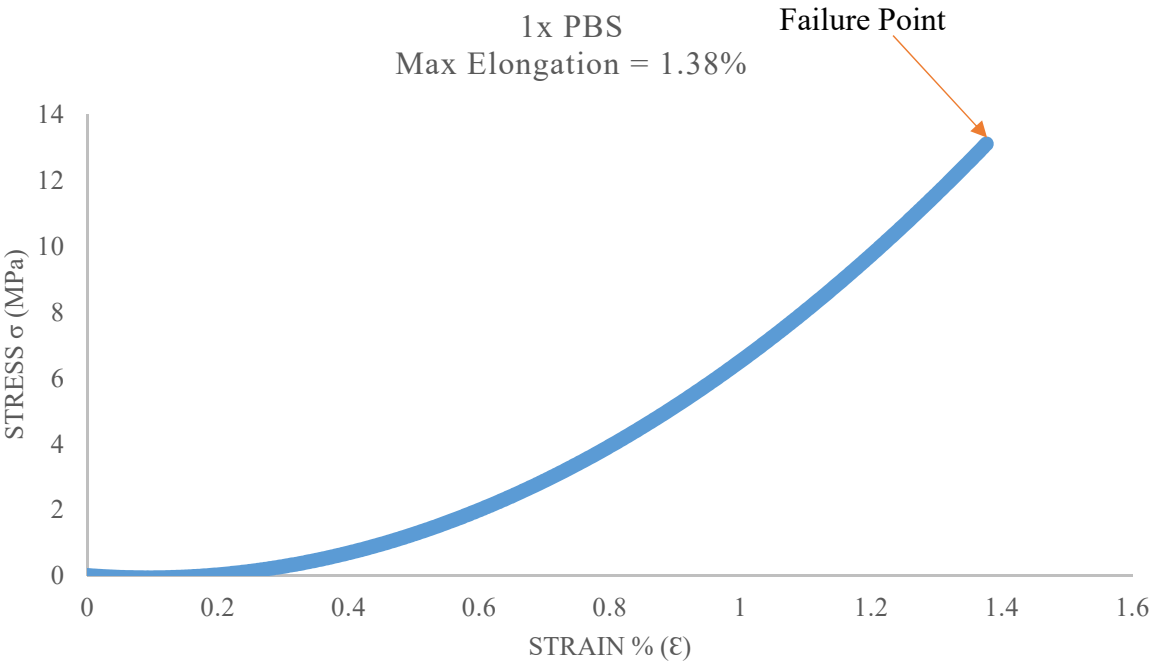

Figure 6-12-One example of the stress- strain curve of the chitosan fiber moisturized using 1x PBS.

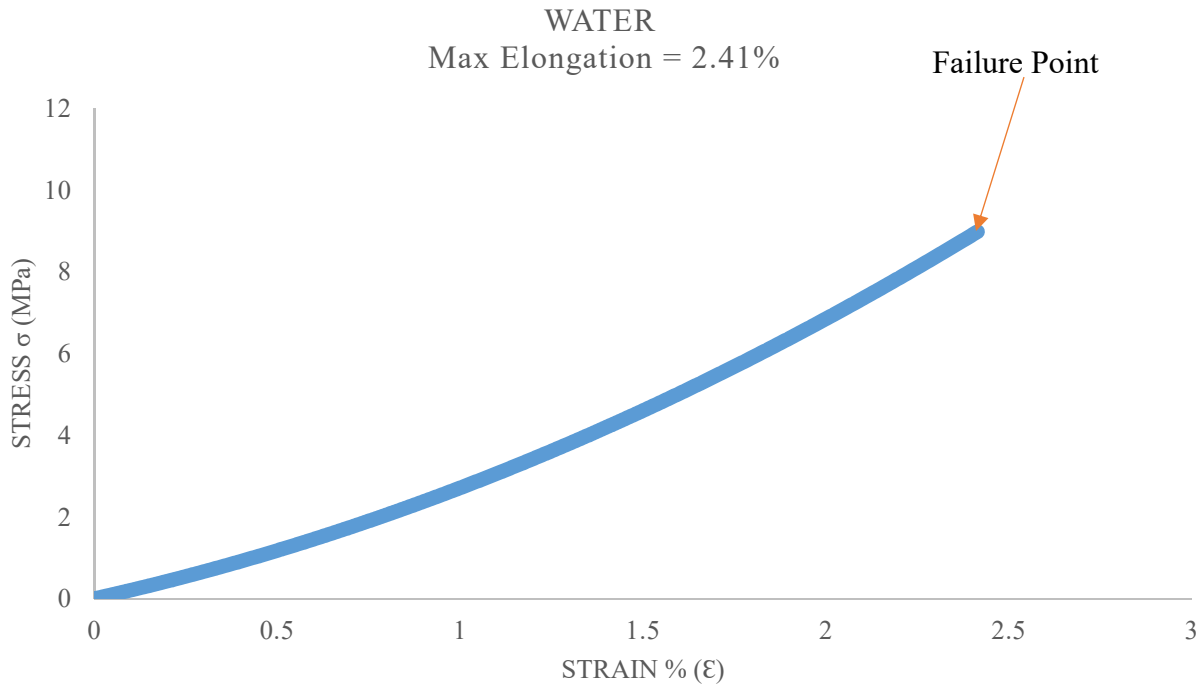

Figure 6-13-One example of the stress-strain curve of the chitosan fiber moisturized using water.

6.5 RHEOLOGY (STORAGE MODULUS)

Tables 6-7 to 6-14 show the results of the rheology for the pure hydrogels (no fiber) and the hydrogels with embedded fibers from each group. The storage modulus for four frequencies, 5, 10, 15, and 20 Hz, are reported. The results are based on frequency sweep at a temperature of 37 ºC, a frequency between 0.1-100 Hz, a strain of 10%, and an initial load of 0.7 N which was recommended by Zuidema et al. [101].

Table 6-7-Storage modulus of the hydrogel (no fiber).

No.	Freq. (Hz)	Storage modulus (Pa)	No.	Freq. (Hz)	Storage modulus (Pa)	No.	Freq. (Hz)	Storage modulus (Pa)	No.	Freq. (Hz)	Storage modulus (Pa)
1	**5**	1472.85	2	**5**	1557.88	3	**5**	1491.66	4	**5**	1338.74
	10	1382.74		**10**	1647.83		**10**	1381.36		**10**	1365.79
	15	1479.88		**15**	1817.04		**15**	1534.29		**15**	1384.44
	20	1617.22		**20**	1849.47		**20**	1739.96		**20**	1431.97

Table 6-8-Storage modulus (mean) for the hydrogel.

Freq. (Hz)	Storage modulus (Pa)	Mean (Pa)	STD Deviation
5	1465.28	1530.82	98.13
10	1444.43		
15	1553.91		
20	1659.66		

Table 6-9-Storage modulus of the 21G group.

No.	Freq. (Hz)	Storage modulus (Pa)	No.	Freq. (Hz)	Storage modulus (Pa)	No.	Freq. (Hz)	Storage modulus (Pa)	No.	Freq. (Hz)	Storage modulus (Pa)
1	**5**	2516.28	2	**5**	3158.90	3	**5**	2269.62	4	**5**	2577.08
	10	2210.74		**10**	3138.54		**10**	2168.61		**10**	2542.63
	15	1933.86		**15**	3107.71		**15**	1936.92		**15**	2513.49
	20	1622.83		**20**	3057.81		**20**	1894.72		**20**	2502.58

Table 6-10-Storage modulus (mean) for the 21G group.

Freq. (Hz)	Storage modulus (Pa)	Mean (Pa)	STD Deviation
5	2630.47	2447.02	158.42
10	2515.13		
15	2372.99		
20	2269.49		

Table 6-11-Storage modulus of the 25G group.

No.	Freq. (Hz)	Storage modulus (Pa)	No.	Freq. (Hz)	Storage modulus (Pa)	No.	Freq. (Hz)	Storage modulus (Pa)	No.	Freq. (Hz)	Storage modulus (Pa)
1	**5**	2348.23	2	**5**	2508.26	3	**5**	1812.02	4	**5**	1886.80
	10	2261.68		**10**	2400.55		**10**	1819.80		**10**	1877.21
	15	2231.78		**15**	2332.30		**15**	1828.11		**15**	1908.28
	20	2148.63		**20**	2256.13		**20**	1864.28		**20**	1941.98

Table 6-12-Storage modulus (mean) for the 25G group.

Freq. (Hz)	Storage modulus (Pa)	Mean (Pa)	STD Deviation
5	2138.83	2089.13	36.47
10	2089.81		
15	2075.12		
20	2052.76		

Table 6-13-Storage modulus of the 27G group.

No.	Freq. (Hz)	Storage modulus (Pa)	No.	Freq. (Hz)	Storage modulus (Pa)	No.	Freq. (Hz)	Storage modulus (Pa)	No.	Freq. (Hz)	Storage modulus (Pa)
1	**5**	1654.00	2	**5**	2189.22	3	**5**	1851.66	4	**5**	1647.12
	10	1701.79		**10**	2238.61		**10**	1744.91		**10**	1448.17
	15	1751.57		**15**	2260.27		**15**	1708.17		**15**	1406.70
	20	1810.15		**20**	2272.85		**20**	1653.54		**20**	1423.80

Table 6-14-Storage modulus (mean) for the 27G group.

Freq. (Hz)	Storage modulus (Pa)	Mean (Pa)	STD Deviation
5	1835.50	1797.66	25.49
10	1783.37		
15	1781.68		
20	1790.09		

6.6 SCANNING ELECTRON MICROSCOPY

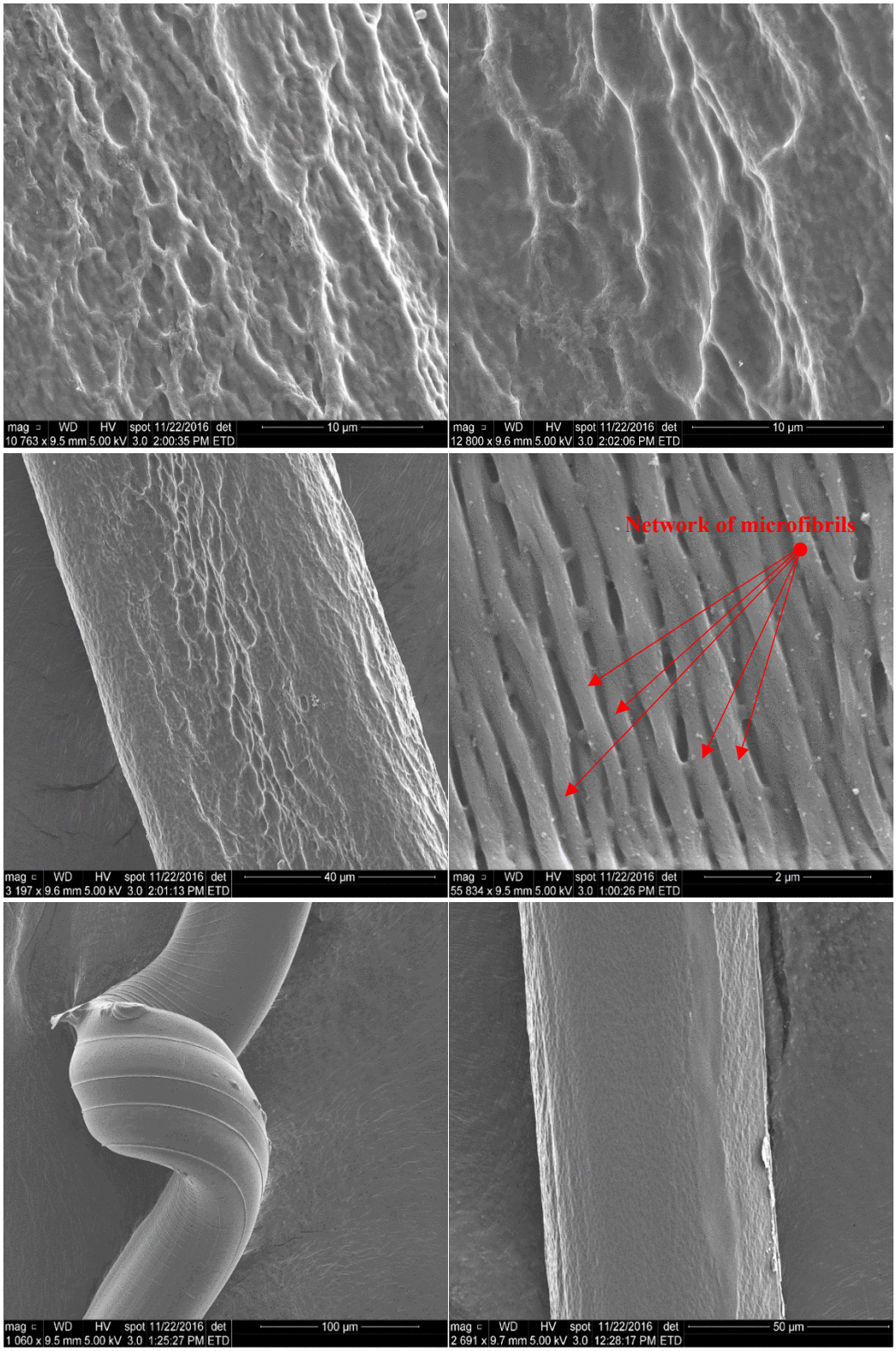

Figure 6-14-Surfaces of the chitosan fibers captured by the scanning electron microscope F-50 with various magnifications.

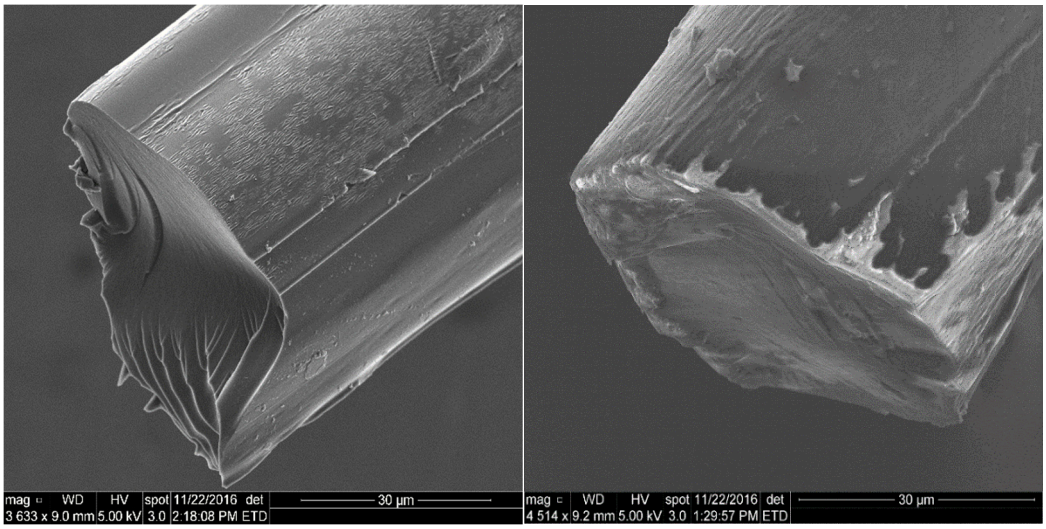

Figure 6-15-Chitosan fiber's cross-section captured by the scanning electron microscope F-50.

The scanning electron microscopy images were used to measure the diameter of the fibers in each group using the software of the SEM. Table 6-15 shows the diameters of the fibers in each group. The error bars in figure 6-16 (the mean values of the diameters) are based on the standard deviations.

Table 6-15-Measured diameter of each group.

27 G	25 G	21 G	
51.20	79.14	126.10	
55.21	77.94	128.20	
55.33	77.84	133.60	
52.36	76.33	131.10	
50.78	77.69	131.08	
47.06	80.36	120.88	
46.39	66.90	123.79	
45.99	68.81	133.99	
45.00	72.27	129.81	
46.59	75.79	128.23	
49.59	75.31	128.68	Mean
3.89	4.50	4.18	SD

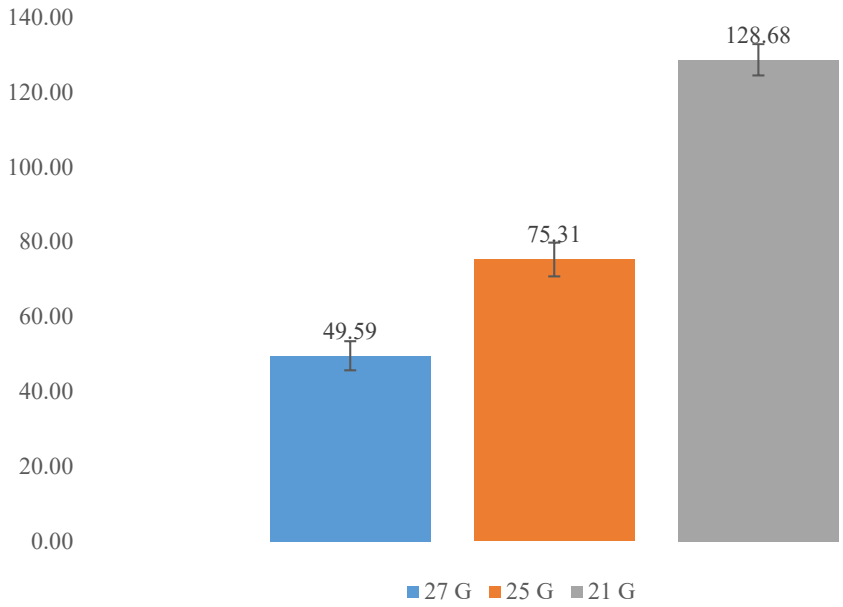

Figure 6-16-Diameter (mean) of the fibers in each group.

The energy-dispersive X-ray spectroscopy result is shown in figure 6-17 which indicates the main components of the fibers. Carbon, Oxygen, and nitrogen are the three main elements which form the chitosan fiber. A negligible amount of NaCl is present in the fiber as well.

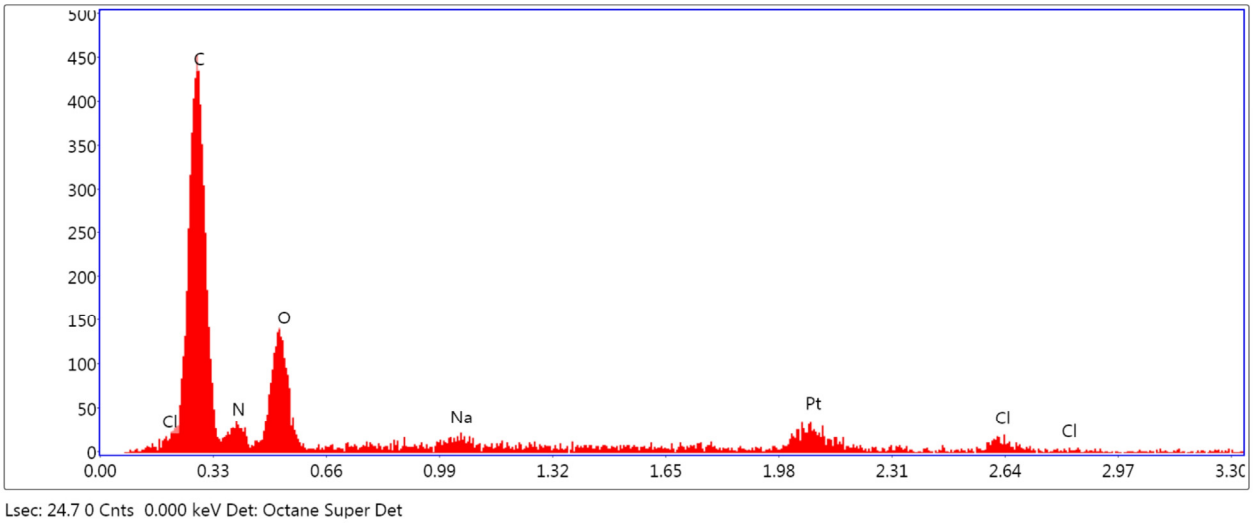

Figure 6-17-Energy-dispersive X-ray spectroscopy result.

6.7 SWELLING CHARACTERISTICS

As mentioned in section 6.6, the fibers in 27G group had the smallest diameter (mean of 50 µm) which was the closet to the fibroblast cells' size (~10-15 microns [104]) among the other groups (25G and 21G). Since the fibers with the smallest diameter are considered to be ultimately introduced to the hydrogel, the swelling experiment was conducted using the fibers from 27G group. Table 6-16 provides the weights (mg) of the empty vials, the vials with the fibers which were placed in each vial, and the vials with the fibers, with the absorbed liquid, at each time point.

Table 6-16-Swelling results at indicated time points. Weights are in milligrams.

Empty Vial	Vial + Fiber	4 h	24 h	72 h	144 h	168 h	
1380.8	1383.0	1407.8	1410.1	1399.0	1399.6	1395.4	
1358.4	1360.8	1396.5	1401.3	1386.6	1381.5	1378.1	
1450.8	1452.4	1463.5	1505.2	1471.4	1480.0	1473.8	
1355.7	1357.6	1357.1	1389.5	1389.0	1383.4	1399.0	
1354.1	1356.3	1385.3	1416.6	1410.3	1388.5	1371.8	
1455.3	1457.7	1484.1	1487.9	1480.6	1472.4	1475.9	
1357.0	1359.0	1375.0	1384.0	1413.8	1380.0	1370.6	
1387.4	1389.5	1409.9	1427.8	1421.5	1412.2	1409.2	Mean

Table 6-17 shows the weights (mg) of the fibers with the absorbed liquids at each time points. These values were obtained by subtracting the weight at each time point from the weight of the empty vial.

Table 6-17-Weight of the fibers with absorbed PBS. Weights are in milligrams.

0h	4h	24h	72h	144h	168h	
2.2	27.0	29.3	18.2	18.8	14.6	
2.4	38.1	42.9	28.2	23.1	19.7	
1.6	12.7	54.4	20.6	29.2	23.0	
1.9	1.4	33.8	33.3	27.7	43.3	
2.2	31.2	62.5	56.2	34.4	17.7	
2.4	28.8	32.6	25.3	17.1	20.6	
2.0	18.0	27.0	56.8	23.0	13.6	
2.1	22.5	40.4	34.1	24.8	21.8	Mean

The mean values of the weights from table 6-17 at each time point are plotted against the time points in figure 6-18.

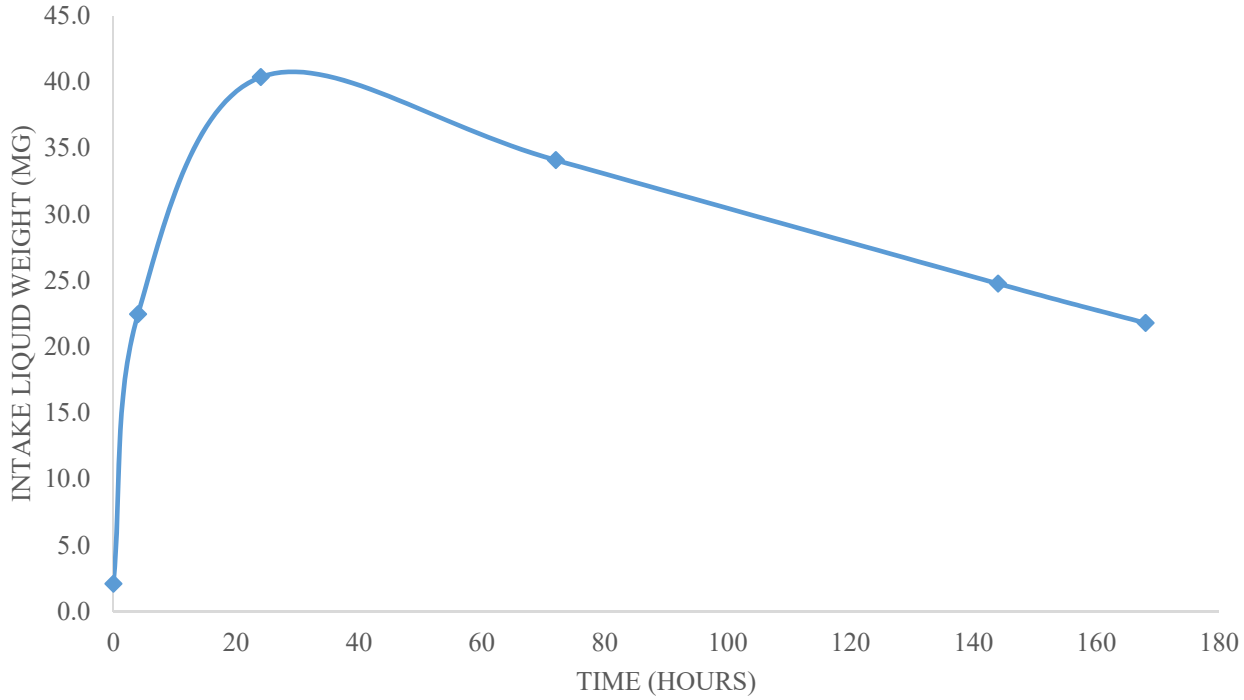

Figure 6-18-Mean values at each time point.

For the swelling ratio shown in table 6-18 (the weight of the fiber with the absorbed liquid, was divided by the weight of the fiber without any liquid).

Table 6-18-Swelling ratio.

0h	4h	24h	72h	144h	168h	
1.0	12.3	13.3	8.3	8.5	6.6	
1.0	15.9	17.9	11.8	9.6	8.2	
1.0	7.9	34.0	12.9	18.2	14.4	
1.0	0.7	17.8	17.5	14.6	22.8	
1.0	14.2	28.4	25.5	15.6	8.0	
1.0	12.0	13.6	10.5	7.1	8.6	
1.0	9.0	13.5	28.4	11.5	6.8	
1.0	10.3	19.8	16.4	12.2	10.8	Mean

The mean values of the swelling ratios at each time point are plotted against the time points in figure 6-19.

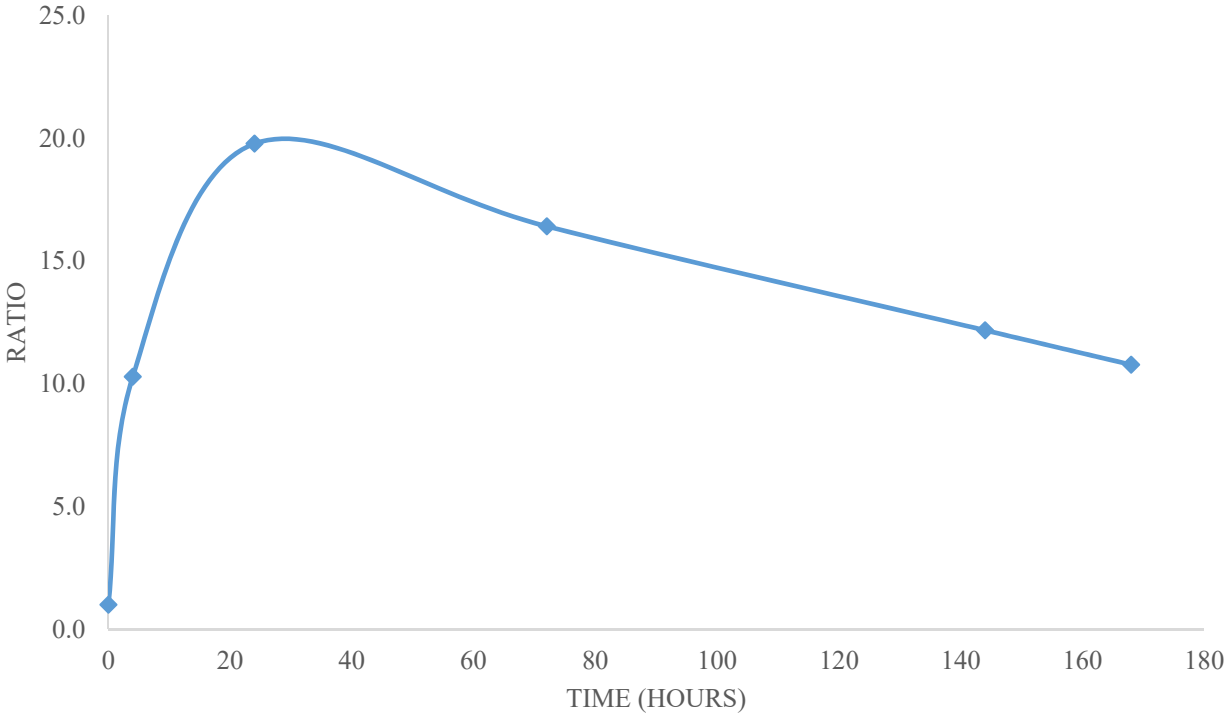

Figure 6-19-Swelling Ratio.

7 DISCUSSION

7.1 VIABILITY

After processing the confocal microscopy data, it was clear that there was no cytotoxicity effect on hVFF due to the cross-linker when glyoxal was diluted to 1 % w/v. On day zero the ratio of live to dead cells was 4 (80% live cells and 20% dead). On day seven, the live to dead ratio decreases to 1.58 (61% live cells and 39% dead). This ratio change, was not caused by the cross-linker of the fiber since the dead cells were distributed evenly throughout the entire gel. Using the cross-linker with a higher concentration than 1% caused many dead cells to appear along the fiber (figure 7-1) regardless of the time point. The live to dead ratio alternation over a week period, might occur due to many reasons, such as lack of CO_2 for some of the encapsulated cells within the hydrogel, and/or homeostasis imbalance.

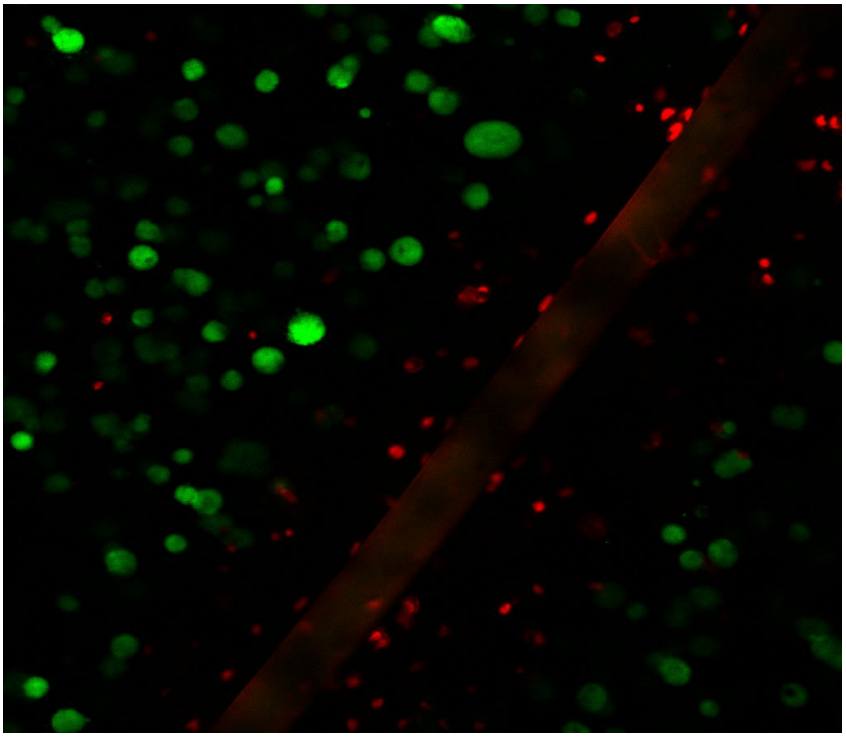

Figure 7-1-Cytotoxicity effect of the cross-linker when used with 10% w/v. Dead cells (red) spread along the fiber.

7.2 MIGRATION

After processing the confocal microscopy data, it was clear that some of the cells moved towards the fiber after 48 hours. The paths of the cells migration, are shown in figure 6-6 with the white arrows generated by the IMARIS software. Despite the promising nature of the obtained results, we do not consider them final and recommend for them to be confirmed using another migration protocol. For the purpose of further investigation, loading the fibers with an agent such as gelatin which attracts cells, is expected to increase the rate of migration.

7.3 TENSILE STRENGTH

The fibers form the three groups (27G, 25G, and 21G) were subjected to the tensile tests. The fibers were tested under three unlike conditions: dry, moisturized with water, and moisturized with 1x PBS.

For each proposed condition, the results of the tensile tests had almost the same pattern and trend regardless of the fibers' diameter (groups), meaning that, the dry fibers in the groups had much higher ultimate strength in comparison with the moisturized conditions regardless of the liquids. The difference in the ultimate strengths was up to a factor of ten between the dry and the moisturized conditions. In the moisturized conditions, although two liquids with different pHs (Water=7, 1x PBS=7.4) were used to moisturize the fibers, the ultimate strengths of the fibers under these two conditions (moisturized) did not vary significantly based on the liquid regardless of the fibers' groups.

As shown in figure 6-10, there was a little difference in terms of the ultimate strengths between the groups (27G, 25G, and 21G) in the case of moisturized with water or moisturized with 1x PBS, however, a significant difference was observed in the dry condition. The mean values of the ultimate strength for 27G, 25G, and 21G were 163.00, 119.20, and 73.60 MPa, respectively. This

difference was due to the size of the fibers in each group. The fibers in the 27G group had the mean diameter of 50 µm while the fibers in the 25G and 21G groups had the mean diameters of 75 µm and 129 µm, respectively. The smaller the volume of a material, the less imperfections and defects are expected to be present within that volume, since less chance is given to defects to emerge when a smaller volume of a material is fabricated [67]. In this study, the strength was increased when the diameter of the fibers was decreased. Also, by reducing the diameter of the fiber more crystalline regions could form and grow causing strength increase.

The results from a few tensile tests were eliminated from the reported data since the obtained values were either too high or too low. This probably was because of either the tensile machine or the table movement during the experiment. Vibration was an issue during the tensile tests, affecting the results directly. Figure 7-2 is an example of abnormal stress-strain curve which was caused by a vibration and was not considered in the reported data.

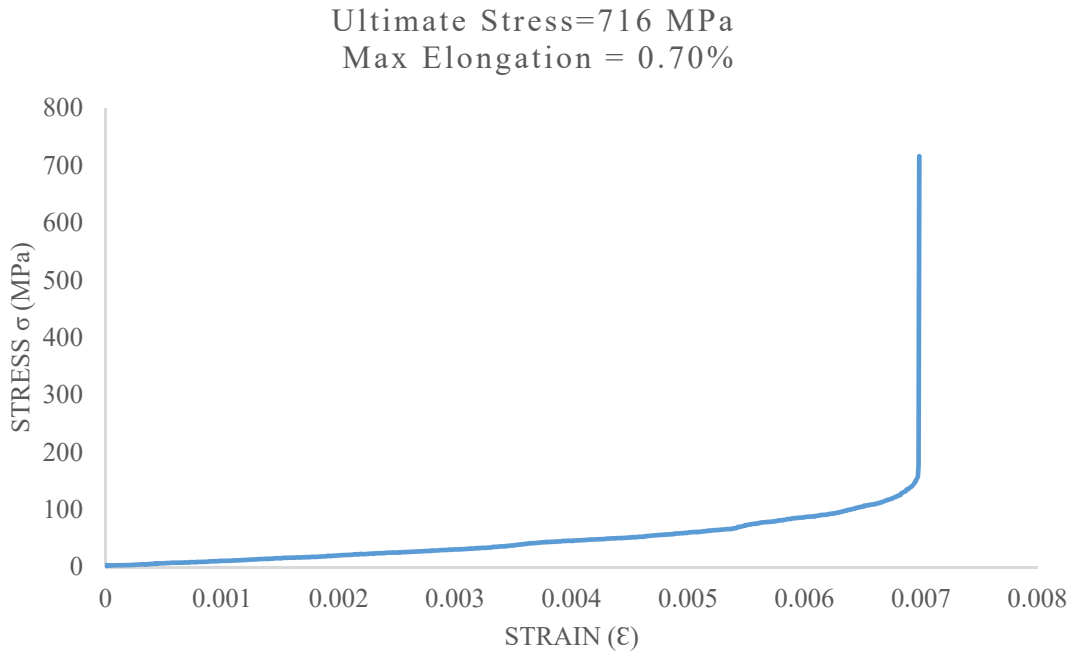

Figure 7-2-Stress-Strain Curve (dry).

7.4 RHEOLOGY (STORAGE MODULUS)

The fibers with a length of 60 cm from each group were segmented and placed randomly inside the gel before curing takes place. Table 7-1 shows the volume fraction of the fibers in the composite material (volume of fibers÷ total volume of a composite) in each group.

Table 7-1-Volume fraction of fiber in each group.

Group	Length of fiber (mm)	Diameter of fiber (µm)	Volume of fiber (mm^3)	Volume of hydrogel (mm^3)	Volume fraction
21G	600	129	7.85	629	0.012
25G	600	75	2.65	629	0.004
27G	600	50	1.18	629	0.002

The reported results in tables 6-7 to 6-14, reveal that the addition of the fibers to the hydrogel significantly altered the mechanical properties of the gel as expected. The highest storage modulus values belong to the 21G group.

The mechanical properties of a composite material depend on orientation, position, and amount of the fibers (volume fraction of fibers) within a composite. The fibers in the 21G group had the largest diameter among the other groups causing the highest volume fraction of the fibers leading to the highest storage modulus.

The variation between the values in each group could be due to different orientation and position of the fibers in the hydrogels since they (fibers) were placed randomly within the gel.

7.5 SCANNING ELECTRON MICROSCOPY (SEM)

As illustrated in figure 6-14, the surfaces of the fibers were not smooth. These slightly rough surfaces might work in favor of the adhesion of the cells. The networks of tiny microfibrils can be seen on the captured images in figure 6-14.

As table 6-15 show, the diameters of the fabricated fibers in each group were smaller than the inner diameter of the needle which was used for the fabrication. These results indicate that the fibers'

diameter with respect to the inner diameter of the needles shrank after crosslinking process due to increasing crystallinity as expected.

7.6 SWELLING CHARACTERISTICS

The swelling tests proved that the chitosan fibers were capable of absorbing the liquid 20 times of their initial weights, within 24 hours. This property makes the chitosan fiber to be a great candidate for being loaded by drugs or growth factors for various drug delivery purposes.

After 24 hours, the weights started to decrease smoothly which might be due to the degradation of the fibers as shown in figure 6-18. After 168 hours (one week), the fibers were still capable of storing the liquid, 10 times of their initial weights.

8 CONCLUSION AND FUTURE WORK

8.1 CONCLUSION

The purpose of this study was to design and fabricate single-strand chitosan fibers to introduce them into the homogenous chitosan hydrogel in order to enhance the mechanical and biological properties of the hydrogel matrix.

The single-strand fibers were fabricated via direct extrusion. The chitosan powder was dissolved in acetic acid to form a 5% w/v solution. The primary solution was then injected to a bath of acetone using a syringe pump. Three groups (21G, 25G, and 27G) based on the needle size were considered for investigation. The smallest possible diameter that we could obtain for the fibers via direct extrusion, had the mean diameter of 50 µm. Glyoxal was used to crosslink the fibers.

The viability tests verified cytotoxicity effect of glyoxal on hVFF cells if used in high concentrations. After dilution of glyoxal to 1 % w/v, no cytotoxicity detected.

Migration of hVFF cells within 48 hours was confirmed through the migration tests.

The tensile tests verified that the fibers have much higher (up to a factor of 10) ultimate strength in the dry condition in comparison with the moisturized conditions. When fibers were moisturized with different liquids in terms of their pHs, almost identical effect was observed. The fibers with the smaller cross-sectional area (diameter) had higher ultimate strengths.

The rheology studies of the composite hydrogel confirmed that the composite hydrogels made from the fibers with the larger diameter (21G) have higher storage modulus since the fiber volume fraction is higher in those composites.

The scanning electron microscopy revealed the rough surfaces of the fibers and the networks of microfibrils. The diameters of the fibers as well as their compositions were obtained by the SEM.

The swelling characterization confirmed the capability of the fibers in storing liquids which is very practical for delivery of drugs and growth factors.

Adding the chitosan fibers to the chitosan hydrogel scaffold was a practical method which enhanced both mechanical and biological properties of the scaffold.

8.2 FUTURE WORK

Some of the factors and parameters in this study might be altered to investigate whether the chitosan fiber can be further optimized.

In terms of fabrication, the temperature of the first solution (chitosan and acetic acid) can be altered to check whether the temperature change affects the fabrication process, since changing the temperature alters the viscosity of the solution. Also, by increasing the temperature, it might be possible to fabricate fibers with a smaller diameter than 50 μm using the same method.

Another factor is an alternative cross-linker instead of glyoxal. Cross-linkers have a great influence on both biological and mechanical properties of the chitosan fiber. Furthermore, concentration of a cross-linker is a critical factor. Since the chitosan fiber comes into contact with the live cells ultimately, the alternative cross-linker must not show any cytotoxicity effects on the cells. The cross-linking time of the fibers can be altered to investigate whether this factor influences the mechanical properties of the fibers.

As it was mentioned before, any concentration more than 1% w/v showed cytotoxicity on hVFF; therefore, all the mechanical tests in this study were performed with the fibers which were cross-linked by 1% w/v glyoxal. If the mechanical properties are the only concern, one might try higher concentrations with this cross-linker or an alternative one. It is reasonable to expect that by increasing the concentration of the cross-linker, the mechanical properties of the fiber improve further.

Lastly, rheology is another test that could be modified. In this study frequency sweep was considered based on the human body temperature (37 ºC). There are many other options to define a rheology study, for instance, time or strain sweep.

BIBLIOGRAPHY

1. Aronson, A.E. and D.M. Bless, Clinical voice disorders. 2009, New York: Thieme.
2. Kent, R.D., MitcogNet, and T. Massachusetts Institute of, The MIT encyclopedia of communication disorders. 2004.
3. Hartnick, C.J. and M.E. Boseley, Clinical management of children's voice disorders. 2010.
4. Klein, A.M. and M.M. Johns, Laryngeal dissection and phonosurgical atlas. 2009.
5. M.D., R.S. Tracheitis. 2014 [cited 2016 09/01]; Available from: http://nethealthbook.com/infectious-disease/respiratory-infections/tracheitis/.
6. Art & Science Graphics. 2015 [cited 2016 9/1]; Available from: http://www.artandsciencegraphics.com/medical-images/.
7. HEALTH & SCIENCE-Understanding Vocal Fold Scarring. 2016 [cited 2016; Available from: http://voicefoundation.org/health-science/voice-disorders/voice-disorders/vocal-fold-scarring/1428-2/.
8. Aronson, A.E., Clinical voice disorders : an interdisciplinary appoarch. 1990, New York; Stuttgart; New York: Thieme ; Georg Thieme Verlag.
9. Blitterswijk, C.A.v. and J.d. Boer, Tissue engineering. 2015.
10. Lanza, R.P., R.S. Langer, and J. Vacanti, Principles of tissue engineering. 2014.
11. Langer, R. and J.P. Vacanti, Tissue engineering. Science (New York, N.Y.), 1993. 260(5110): p. 920-6.
12. Migonney, V., Biomaterials. 2014.
13. Wong, J.Y. and J.D. Bronzino, Biomaterials. 2007.
14. Shi, D., Introduction to biomaterials. 2006.
15. Joint U.S.-Japan Seminar on Advances in Chitin, C., E. Related, and J.P. Zikakis. Chitin, chitosan, and related enzymes. Orlando: Academic Press.
16. Kim, S.-K., Chitin and chitosan derivatives : advances in drug discovery and developments. 2014.
17. Dutta, P.K., J. Dutta, and V. S. Tripathi, Chitin and chitosan: Chemistry, properties and applications. Journal of Scientific and Industrial Research, 2004. 63(1): p. 20-31.
18. Kurita, K., Chemistry and application of chitin and chitosan. Polymer Degradation and Stability, 1998. 59(1): p. 117-120.
19. Peter, M.G., Applications and environmental aspects of chitin and chitosan. Journal of Macromolecular Science, Part A: Pure and Applied Chemistry, 1995. 32(4): p. 629-640.
20. Pillai, C.K.S., W. Paul, and C. P. Sharma, Chitin and chitosan polymers: Chemistry, solubility and fiber formation. Progress in Polymer Science, 2009. 34(7): p. 641-678.
21. Ravi Kumar, M.N.V., A review of chitin and chitosan applications. Reactive and Functional Polymers, 2000. 46(1): p. 1-27.
22. Rinaudo, M., Chitin and chitosan: Properties and applications. Progress in Polymer Science 2006. 31(7): p. 603-632.
23. Venkatesan, J.a.S.-K.K., Chitosan composites for bone tissue engineering— An overview. Marine Drugs, 2010. 8(8): p. 2252-2266.
24. Sahib, W., Chitosan chemical structural formula.svg. 25 May 2014.

25. Cao, Z., H. Xu, R. Tang, W. Wei, and W. Xu, Synthesis, characterization and molluscicidal activity of triphenyltin phosphorylated chitosan. Chemistry Bulletin/Huaxue Tongbao 2008. 71(7): p. 528-532.
26. Cárdenas, G., G. Cabrera, E. Taboada, and M. Rinaudo, Synthesis and characterization of chitosan alkyl phosphate. Journal of the Chilean Chemical Society, 2006. 51(1): p. 815-820.
27. Chesnutt, B.M., Y. Yuan, N. Brahmandam et al., Characterization of biomimetic calcium phosphate on phosphorylated chitosan films. ournal of Biomedical Materials Research-Part A, 2007. 82(2): p. 343-353.
28. Datta, P., S. Dhara, and J. Chatterjee, Hydrogels and electrospun nanofibrous scaffolds of N -methylene phosphonic chitosan as bioinspired osteoconductive materials for bone grafting. Carbohydrate Polymers, 2012. 87(2): p. 1354-1362.
29. Fan, L., P. Wu, J. Zhang et al, Synthesis and anticoagulant activity of the quaternary ammonium chitosan sulfates. International Journal of Biological Macromolecules, 2012. 50(1): p. 31-37.
30. Gamzazade, A., A. Sklyar, S. Nasibov, I. Sushkov, A. Shashkov, and Yu Knirel, Structural features of sulfated chitosans. Carbohydrate Polymers, 1997. 34(1-2): p. 113-116.
31. Hirano, S., Y. Tanaka, M. Hasegawa, K. Tobetto, and A. Nishioka, Effect of sulfated derivatives of chitosan on some blood coagulant factors. Carbohydrate Research, 1985. 137(C): p. 205-215.
32. Jayakumar, R., R. L. Reis, and J. F. Mano, Chemistry and applications of phosphorylated chitin and chitosan. E-Polymers, 2006. 35: p. 1-16.
33. Jayakumar, R., N. Nwe, S. Tokura, and H. Tamura, Sulfated chitin and chitosan as novel biomaterials. International Journal of Biological Macromolecules, 2007. 40(3): p. 175-181.
34. Jayakumar, R., H. Nagahama, T. Furuike, and H. Tamura, Synthesis of phosphorylated chitosan by novel method and its characterization. International Journal of Biological Macromolecules, 2008a. 42(4): p. 335-339.
35. Jayakumar, R., N. Selvamurugan, S. V. Nair, S. Tokura, and H. Tamura, Preparative methods of phosphorylated chitin and chitosan— An overview. International Journal of Biological Macromolecules, 2008b. 43(3): p. 221-225.
36. Je, J.Y., E. K. Kim, C. B. Ahn et al, Sulfated chitooligosaccharides as prolyl endopeptidase inhibitor. International Journal of Biological Macromolecules, 2007. 41(5): p. 529-533.
37. Karadeniz, F., M. Z. Karagozlu, S. Y. Pyun, and S. K. Kim, Sulfation of chitosan oligomers enhances their anti-adipogenic effect in 3T3-L1 adipocytes. Carbohydrate Polymers, 2011. 86(2): p. 666-671.
38. Kornilaeva, G.V., T. V. Makarova, A. I. Gamzazade, A. M. Sklyar, S. M. Nasibov, and E. V. Karamov, Sulphated chitosan derivatives as HIV-infection inhibitors. Immunologiya 1995. 1(1): p. 13-16.
39. Li, B., L. Huang, X. Wang, J. Ma, and F. Xie, Biodegradation and compressive strength of phosphorylated chitosan/chitosan/hydroxyapatite bio-composites. Materials and Design, 2011. 32(8-9): p. 4543-4547.
40. Li, B., L. Huang, X. Wang, J. Ma, F. Xie, and L. Xia, Effect of micropores and citric acid on the bioactivity of phosphorylated chitosan/chitosan/hydroxyapatite composites. Ceramics International, 2013. 39(3): p. 3423-3427.

41. Li, Q.L., Z. Q. Chen, B. W. Darvell et al., Biomimetic synthesis of the composites of hydroxyapatite and chitosan-phosphorylated chitosan polyelectrolyte complex. Materials Letters 2006. 60(29-30): p. 3533-3536.
42. Li, Q.L., Z. Q. Chen, B. W. Darvell et al. , Chitosan-phosphorylated chitosan polyelectrolyte complex hydrogel as an osteoblast carrier. Journal of Biomedical Materials Research— Part B Applied Biomaterials, 2007a. 82(2): p. 481-486.
43. Li, Q.L., N. Huang, Z. Chen, and X. Tang, Biomimetic synthesis of the nanocomposite of phosphorylated chitosan and hydroxyapatite and its bioactivity in vitro. Key Engineering Materials, 2007b. 330-332(19): p. 721-724.
44. Liu, J., Y. Zheng, W. Wang, and A. Wang, Preparation and swelling properties of semi-IPN hydrogels based on chitosan-g-poly(acrylic acid) and phosphorylated polyvinyl alcohol. Journal of Applied Polymer Science, 2009. 114(1): p. 643-652.
45. Lu, X., H. Guo, L. Sun, L. Zhang, and Y. Zhang, Protective effects of sulfated chitooligosaccharides with different degrees of substitution in MIN6 cells. International Journal of Biological Macromolecules, 2013. 52(1): p. 92-98.
46. Ma, B., W. Huang, W. Kang, and J. Yan, Studies on preparation of sulfated derivatives of chitosan from mucor rouxianus. Lizi Jiaohuan Yu Xifu/Ion Exchange and Adsorption, 2007. 23(5): p. 451-458.
47. Mariappan, M.R., E. A. Alas, J. G. Williams, and M. D. Prager, Chitosan and chitosan sulfate have opposing effects on collagen– fibroblast interactions. Wound Repair and Regeneration 1999. 7(5): p. 400-406.
48. Miao, J., and G. Chen, Sulfated chitosan (SCS)/polysulfone (PS) composite nanofiltration membrane surface cross-linked by epichlorohydrin. 2012.
49. Muzzarelli, R.A.A., F. Tanfani, M. Emanuelli, D. P. Pace, E. Chiurazzi, and M. Piani, Sulfated N -(carboxymethyl)chitosans: Novel blood anticoagulants. Carbohydrate Research, 1984. 126(2): p. 225-231.
50. Pires, N.R., P. L. R. Cunha, J. S. MacIel et al, Sulfated chitosan as tear substitute with no antimicrobial activity. Carbohydrate Polymers, 2013. 91(1): p. 92-99.
51. Ryzhenkov, V.E., M. A. Solovyeva, O. V. Remesova, and I. V. Okunevich, Hypolipidemic action of sulfated polysaccharides. Voprosy Meditsinskoj Khimii, 1996. 42(2): p. 118-119.
52. Saiki, I., J. Murata, M. Nakajima, S. Tokura, and I. Azuma, Inhibition by sulfated chitin derivatives of invasion through extracellular matrix and enzymatic degradation by metastatic melanoma cells. Cancer Research, 1990. 50(12): p. 3631-3637.
53. Shelma, R.a.C.P.S., Development of lauroyl sulfated chitosan for enhancing hemocompatibility of chitosan. Colloids and Surfaces B: Biointerfaces, 2011. 84(2): p. 561-570.
54. Srakaew, V., P. Ruangsri, K. Suthin, P. Thunyakitpisal, and W. Tachaboonyakiat, Sodium-phosphorylated chitosan/zinc oxide complexes and evaluation of their cytocompatibility: An approach for periodontal dressing. Journal of Biomaterials Applications, 2012. 27(4): p. 403-412.
55. Vongchan, P., W. Sajomsang, D. Subyen, and P. Kongtawelert, Anticoagulant activity of a sulfated chitosan. Carbohydrate Research, 2002. 337(13): p. 1239-1242.
56. Wang, K., H. Li, Q. Ye et al., Synthesis and anticoagulant action of sulfated chitosan/Eu 2O 3 nano-oxides hybrid materials. Zhongguo Xitu Xuebao/Journal of the Chinese Rare Earth Society, 2011. 29(6): p. 764-768.

57. Xing, R., S. Liu, H. Yu, Q. Zhang, Z. Li, and P. Li, Preparation of low-molecular-weight and highsulfate-content chitosans under microwave radiation and their potential antioxidant activity in vitro. Carbohydrate Research, 2004. 339(15): p. 2515-2519.
58. Xing, R., H. Yu, S. Liu et al., Antioxidant activity of differently regioselective chitosan sulfates in vitro. Bioorganic and Medicinal Chemistry, 2005. 13(4): p. 1387-1392.
59. Yang, J., K. Luo, D. Li et al., Preparation, characterization and in vitro anticoagulant activity of highly sulfated chitosan. International Journal of Biological Macromolecules, 2013. 52(1): p. 25-31.
60. Yang, Y., Y. Zhou, W. Hou, Y. Zhao, and Y. Ren, Preparation and anticoagulant activity of sulfated 6-carboxychitosan. 2008.
61. Yeh, H.Y.a.J.C.L., Surface phosphorylation for polyelectrolyte complex of chitosan and its sulfonated derivative: Surface analysis, blood compatibility and adipose derived stem cell contact properties. Journal of Biomaterials Science, Polymer Edition, 2012. 23(1-4): p. 233-250.
62. Zhang, C., Q. Ping, H. Zhang, and J. Shen, Preparation of N-alkyl-O-sulfate chitosan derivatives and micellar solubilization of taxol. Carbohydrate Polymers, 2003. 54(2): p. 137-141.
63. Zhao, D., J. Xu, L. Wang et al., Study of two chitosan derivatives phosphorylated at hydroxyl or amino groups for application as flocculants. Journal of Applied Polymer Science, 2012. 125(SUPPL. 2): p. E299– E305.
64. Zhou, H., J. Qian, J. Wang et al., Enhanced bioactivity of bone morphogenetic protein-2 with low dose of 2-N, 6-O-sulfated chitosan in vitro and in vivo. Biomaterials, 2009. 30(9): p. 1715-1724.
65. Campbell, F.C., Structural composite materials. 2010.
66. Harris, B. and M. Institute of, Engineering composite materials. 1999.
67. Hoa, S.V., Principles of the manufacturing of composite materials. 2009.
68. Davim, J.P., Materials and Manufacturing Technology : Drilling of Composite Materials. 2009, New York, US: Nova.
69. Li, Z., H. R. Ramay, K. D. Hauch, D. Xiao, and M. Zhang, Chitosan– alginate hybrid scaffolds for bone tissue engineering. Biomaterials, 2005. 26(28): p. 3919-3928.
70. Tan, W., R. Krishnaraj, and T. A Desai, Evaluation of nanostructured composite collagen–chitosan matrices for tissue engineering. Tissue Engineering, 2001. 7(2): p. 203-210.
71. Zhang, Y.a.M.Z., Calcium phosphate/chitosan composite scaffolds for controlled in vitro antibiotic drug release. Journal of Biomedical Materials Research-Part A, 2002. 62(3): p. 378-386.
72. Kong, L., Y. Gao, W. Cao, Y. Gong, N. Zhao, and X. Zhang, Preparation and characterization of nano-hydroxyapatite/chitosan composite scaffolds. Journal of Biomedical Materials Research Part A, 2005. 75(2): p. 275-282.
73. Huang, R.Y.M., R. Pal, and G. Y. Moon, Crosslinked chitosan composite membrane for the pervaporation dehydration of alcohol mixtures and enhancement of structural stability of chitosan/polysulfone composite membranes. Journal of Membrane Science, 1999. 160(1): p. 17-30.
74. Yang J, C.T., Nagaoka M, Goto M, Cho CS, Akaike T Hepatocyte-specific porous polymer-scaffolds of alginate/galactosylated chitosan sponge for liver-tissue engineering. Biotechnol Lett, 2001. 23: p. 1385–1389.
75. Dutta, P.K., Chitin and chitosan for regenerative medicine. 2016.

76. Tiwari, A., M.R. Alenezi, and S.C. Jun, Advanced composite materials. 2016.
77. Douroumis, D., Hot-melt extrusion : pharmaceutical applications. 2012.
78. Gupta, H.N., Manufacturing Process. 2009.
79. Bauser, M., G. Sauer, and K. Siegert, Extrusion. 2006.
80. Lafleur, P.G. and B. Vergnes, Polymer extrusion. 2014.
81. Walczak, Z.K., Processes of fiber formation. 2002.
82. A.B. Dessai, G.L.W., Polymer Sci., Symposia, 1974. 46: p. 291.
83. D.C. Basset, A.K., S. Nitsuhashi, Polymer Sci., 1963 A1 p. 763.
84. Geil, P.H., Polymer Single CrystalsInterscience Publ. 1963: p. 86.
85. H.A. Lanceley, A.S., Makromol. Chem. 1966. 94: p. 30.
86. H.D. Keith, E.J.P.J., Appl. Phys., 1963. 34: p. 2409.
87. J.G. Fatou, E.R., R. Garcia Valdecasas, Polymer Sci., (Phys.), 1975(13): p. 2103.
88. Mandelkern, L., Growth and Perfection of Crystals. John Wiley and Sons, 1958: p. 490.
89. Zhang, D., Advances in filament spinning of polymers and textiles. 2014.
90. Judawisastra, H., I.O.C. Hadyiswanto, and W. Winiati, The Effects of Demineralization Process on Diameter, Tensile Properties and Biodegradation of Chitosan Fiber. Procedia Chemistry Procedia Chemistry, 2012. 4(6): p. 138-145.
91. Tokura, S., N. Nishi, and J. Noguchi, Studies on Chitin. III. Preparation of Chitin Fibers. Polym J Polymer Journal, 1979. 11(10): p. 781-786.
92. Hirano, S., et al., Wet spun chitosan-collagen fibers, their chemical N-modifications, and blood compatibility. JBMT</cja:jid> Biomaterials, 2000. 21(10): p. 997-1003.
93. Albanna, M.Z., et al., Chitosan fibers with improved biological and mechanical properties for tissue engineering applications. Journal of the Mechanical Behavior of Biomedical Materials Journal of the Mechanical Behavior of Biomedical Materials, 2013. 20(9): p. 217-226.
94. Yang, Q., et al., Studies of cross-linking reaction on chitosan fiber with glyoxal. CARP Carbohydrate Polymers, 2005. 59(2): p. 205-210.
95. Probes, M., LIVE/DEAD ® Viability/Cytotoxicity Kit *for mammalian cells, M.P. Inc., Editor. 21-12-2005. p. 7.
96. Probes, M., Cell labeling solution. 2011.
97. Callister, W.D. and D.G. Rethwisch, Fundamentals of materials science and engineering : an integrated approach. 2008, Hoboken, NJ: John Wiley & Sons.
98. Davis, J.R., Tensile testing. 2004.
99. Morrison, F.A., Understanding rheology. 2001.
100. Irgens, F., Rheology and non-Newtonian fluids. 2013.
101. Zuidema, J.M., et al., A protocol for rheological characterization of hydrogels for tissue engineering strategies. Journal of biomedical materials research. Part B, Applied biomaterials, 2014. 102(5): p. 1063-73.
102. Zhou, W. and Z.L. Wang, Scanning microscopy for nanotechnology : techniques and applications. 2007.
103. Schema_MEB_(it).svg: User:Steff, m.b.U.A. Diagram of a scanning electron microscope with English captions. 3 March 2010 [cited 2016; Available from: https://commons.wikimedia.org/wiki/File:Schema_MEB_(en).svg.
104. Jr., R.A.F., Nanomedicine. Landes Biosciencee, Georgetown, TX, 1999. I(Basic Capabilities).

105. Gatford, J. A diagram of the electrospinning process showing the onset of instability. 8 September 2008; Available from: https://commons.wikimedia.org/wiki/File:Electrospinning_Diagram.jpg.

9 APPENDIX

For this study, various manufacturing methods were considered. First, electrospinning was selected as an option. Electrospinning machine works with high voltage which causes polymer solution to be charged, electrostatic repulsion then offsets the surface tension on the tip of the needle, therefore, the solution can stretch. Figure 9-1 demonstrates the setup of an electrospinning machine.

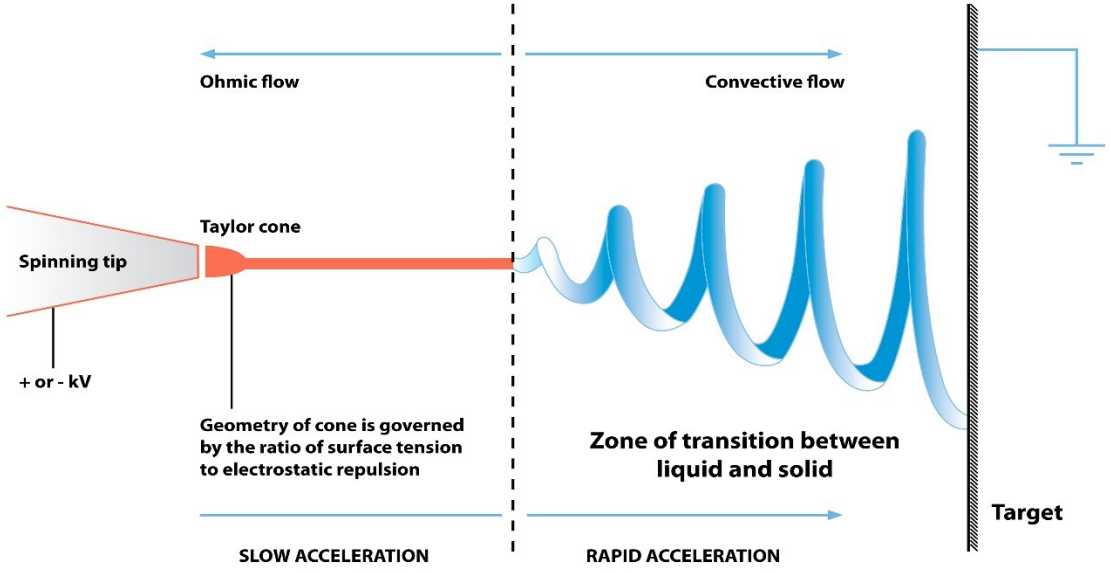

Figure 9-1-A schematic of an electrospinning machine, Joanna Gatford, Wikimedia, (https://commons.wikimedia.org/wiki/File:Electrospinning_Diagram.jpg) [105].

There were two serious challenges with this method which needed to be addressed for fabrication of single-strand chitosan fibers. First challenge was to find a host solvent for chitosan to be so volatile. The reason was to collect pure fibers on the surface of the collector and not the solvent, therefore, the host solvent had to be volatile enough to be vaporized before reaching to the collector. Acetic acid was selected since it is a great candidate to solve chitosan, however, this acid was not volatile enough and consequently could easily reach to the surface and damage the fibers.

On the other hand, fibers that are obtained by this manufacturing method are not individual fibers. The product of this method is a sheet of fibers which are not separable after fabrication. As a result, further investigation on electrospinning were terminated since these fibers were not injectable and the research objective could not be met.